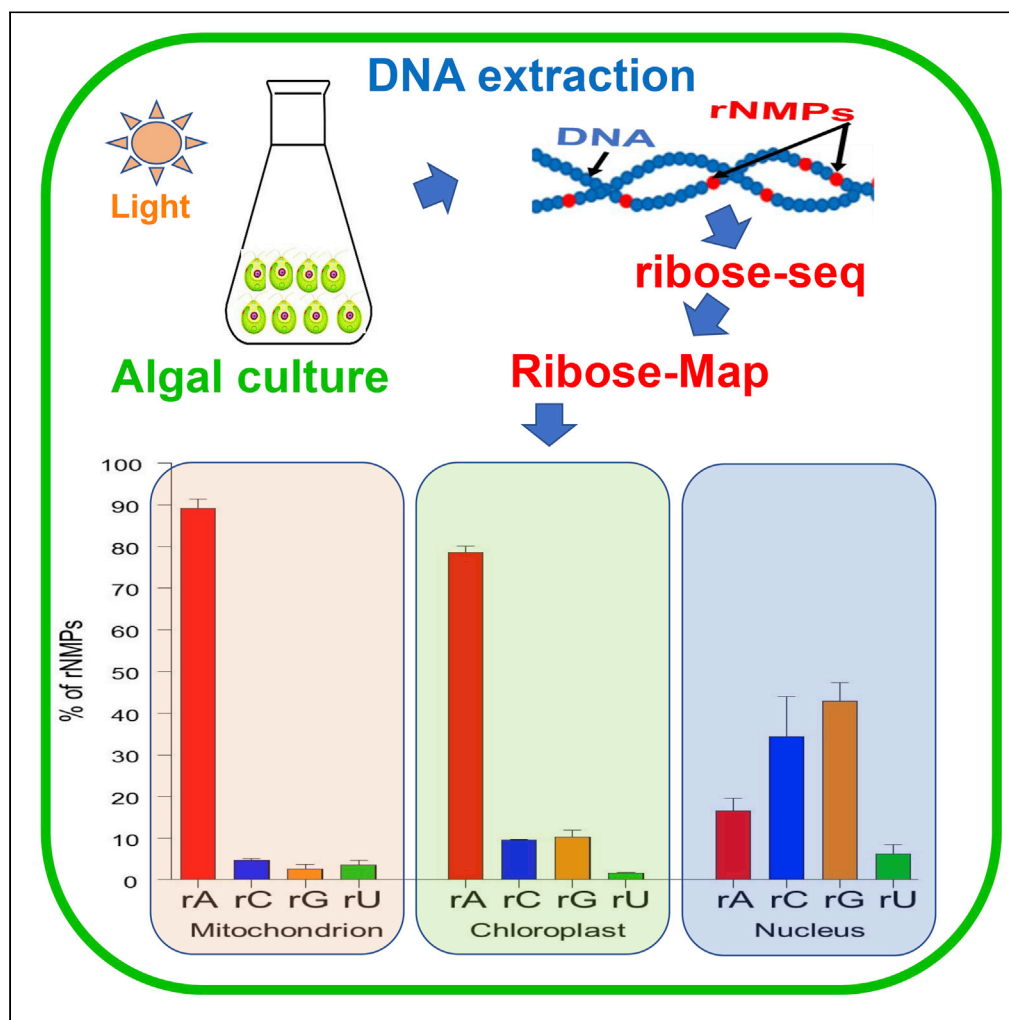


## Article

Disproportionate presence of adenosine in mitochondrial and chloroplast DNA of *Chlamydomonas reinhardtii*

Waleed M.M. El-Sayed, Alli L. Gombolay, Penghao Xu, ..., Baek Kim, Yongsheng Chen, Francesca Storici

storici@gatech.edu

## HIGHLIGHTS

The sites of ribonucleotides embedded in *Chlamydomonas reinhardtii* DNA are revealed

Adenosine is disproportionately abundant in algal mitochondrial and chloroplast DNA

There is a high ATP level present in the algal cells

*C. reinhardtii* orthologous genes for the three subunits of ribonuclease H2 are found

## Article

Disproportionate presence of adenosine  
in mitochondrial and chloroplast  
DNA of *Chlamydomonas reinhardtii*

Waleed M.M. El-Sayed,<sup>1,2,3</sup> Alli L. Gombolay,<sup>1,7</sup> Penghao Xu,<sup>1,7</sup> Taehwan Yang,<sup>1,7</sup> Youngkyu Jeon,<sup>1,7</sup> Sathya Balachander,<sup>1,7</sup> Gary Newnam,<sup>1</sup> Sijia Tao,<sup>4</sup> Nicole E. Bowen,<sup>4</sup> Tomáš Brůna,<sup>1</sup> Mark Borodovsky,<sup>1,5,6</sup> Raymond F. Schinazi,<sup>4</sup> Baek Kim,<sup>4</sup> Yongsheng Chen,<sup>2</sup> and Francesca Storici<sup>1,8,\*</sup>

## SUMMARY

**Ribonucleoside monophosphates (rNMPs) represent the most common non-standard nucleotides found in the genome of cells. The distribution of rNMPs in DNA has been studied only in limited genomes. Using the ribose-seq protocol and the Ribose-Map bioinformatics toolkit, we reveal the distribution of rNMPs incorporated into the whole genome of a photosynthetic unicellular green alga, *Chlamydomonas reinhardtii*. We discovered a disproportionate incorporation of adenosine in the mitochondrial and chloroplast DNA, in contrast to the nuclear DNA, relative to the corresponding nucleotide content of these *C. reinhardtii* organelle genomes. Our results demonstrate that the rNMP content in the DNA of the algal organelles reflects an elevated ATP level present in the algal cells. We reveal specific biases and patterns in rNMP distributions in the algal mitochondrial, chloroplast, and nuclear DNA. Moreover, we identified the *C. reinhardtii* orthologous genes for all three subunits of the RNase H2 enzyme using GeneMark-EP + gene finder.**

## INTRODUCTION

The presence of ribose sugar in place of deoxyribose in DNA is a common DNA modification due to the abundant incorporation of ribonucleoside monophosphates (rNMPs), which are the units of RNA, by DNA polymerases (Nava et al., 2020; Williams et al., 2016). While it has been known for a long time that rNMPs are present in specific DNA sequences, such as mouse and human mitochondrial DNA (Grossman et al., 1973), at the mating type locus in the nuclear DNA of fission yeast (Vengrova and Dalgaard, 2006) and even in chloroplast DNA (Kolodner et al., 1975), only in the last decade has the ribose in DNA been defined as the most abundant alteration in the DNA of cells (Caldecott, 2014; Cavanaugh et al., 2010; Clausen et al., 2013; Gosavi et al., 2012; Kasiviswanathan and Copeland, 2011; Kennedy et al., 2012; Lemor et al., 2018; McDonald et al., 2012; Nick McElhinny et al., 2010; Potenski and Klein, 2014; Williams and Kunkel, 2014; Williams et al., 2016). Recent studies highlight the capacity of many DNA polymerases to incorporate rNMPs into DNA (Astatke et al., 1998; Bonnin et al., 1999; Brown and Suo, 2011; Cavanaugh et al., 2010; Gong et al., 2005; Kasiviswanathan and Copeland, 2011; Kennedy et al., 2012; McDonald et al., 2012; Nick McElhinny and Ramsden, 2003; Patel and Loeb, 2000). For example, *Escherichia coli* polymerase V (McDonald et al., 2012), the polymerase component of bacterial non-homologous end joining ligases (Zhu and Shuman, 2008), all replicative polymerases of budding yeast (Pol  $\alpha$ ,  $\delta$ , and  $\epsilon$ ) (Nick McElhinny et al., 2010), and the human replicative polymerase  $\delta$  (Clausen et al., 2013) can insert rNMPs into DNA. Human DNA polymerases  $\lambda$  and  $\mu$  can insert rNMPs with the same efficiency as deoxyribonucleoside monophosphates (dNMPs) (Gosavi et al., 2012; Moon et al., 2017). In addition, the reverse transcriptase of the human immunodeficiency virus inserts 1 rNMP per 146 dNMPs in the viral genome before integrating into human macrophage DNA (Kennedy et al., 2012). Although these data suggest that rNMPs in DNA are broadly present in nature, studies examining primarily the positions, patterns, and hotspots of rNMPs in DNA have only been done for yeast genomic DNA (Balachander et al., 2020; Clausen et al., 2015; Daigaku et al., 2015; Jinks-Robertson and Klein, 2015; Koh et al., 2015; Reijns et al., 2015). Because ribonuclease (RNase) H2 is the major enzyme removing rNMPs from DNA (Sparks et al., 2012), the initial mapping of rNMPs in DNA to a single-nucleotide resolution was done in yeast strains with non-functional RNase H2

<sup>1</sup>School of Biological Sciences, Georgia Institute of Technology, Atlanta, GA 30332, USA

<sup>2</sup>School of Civil and Environmental Engineering, Georgia Institute of Technology, Atlanta, GA 30332, USA

<sup>3</sup>Marine Microbiology Department, National Institute of Oceanography and Fisheries, Red Sea, 84517, Egypt

<sup>4</sup>Department of Pediatrics, School of Medicine, Emory University, Atlanta, GA 30309, USA

<sup>5</sup>Wallace H. Coulter Department of Biomedical Engineering, Georgia Institute of Technology, Atlanta, GA 30332, USA

<sup>6</sup>School of Computational Science and Engineering, Georgia Institute of Technology, Atlanta, GA 30332, USA

<sup>7</sup>These authors contributed equally

<sup>8</sup>Lead Contact

\*Correspondence: storici@gatech.edu

<https://doi.org/10.1016/j.isci.2020.102005>



(Clausen et al., 2015; Daigaku et al., 2015; Jinks-Robertson and Klein, 2015; Koh et al., 2015; Reijns et al., 2015). Moreover, several reports have shown that RNase H2 is not active in yeast and human mitochondrial DNA (Balachander et al., 2020; Berglund et al., 2017; Wanrooij et al., 2017). This likely explains why, using a collection of *Saccharomyces cerevisiae* mutants with altered nucleotide pool composition, it was shown that variations in the deoxynucleotide triphosphate (dNTP) pool can significantly affect the rNMP-incorporation frequency of mitochondrial DNA either in wild-type or in RNase H2-defective cells, but not that of nuclear DNA in wild-type RNase H2 cells (Wanrooij et al., 2017). Similarly, depletion of dNTP pools promoted rNMP incorporation in human mitochondrial DNA (Berglund et al., 2017). While nucleotide pool imbalances certainly play a major role in rNMP composition in genomic DNA, there are factors beyond variation in nucleotide pools that affect distribution and patterns of rNMP incorporation in DNA. Recently, by studying rNMP profiles in the genomes of three yeast species (*S. cerevisiae*, *Saccharomyces paradoxus*, and *Schizosaccharomyces pombe*) and several different strains of these yeasts having either wild-type or mutant RNase H2, we showed low levels of rU in the mitochondrial DNA as well as in the nuclear DNA of RNase H2-defective cells of all three yeast species, as well as dominant rC and low rG in the nuclear DNA of wild-type RNase H2 cells of all three yeast species (Balachander et al., 2020). We further observed non-uniform distribution in both the yeast nuclear and mitochondrial DNA, uncovering that the dNMP immediately upstream of the rNMP has a strong impact on the pattern of rNMP incorporation in mitochondrial as well as nuclear yeast DNA (Balachander et al., 2020).

The inclusion of rNMPs in DNA alters its stability, structure, plasticity, and ability to interact with proteins (Chiu et al., 2014; Klein, 2017). The presence of rNMPs in DNA may also regulate/modulate cellular functions and if conserved could manifest some type of epigenetic interaction in the cell. Thus, it is important to map rNMP sites in DNA and to characterize their features and rules of incorporation to understand the biological significance of rNMPs in DNA and determine whether these features and rules are conserved across different organisms or cell types. Our molecular and computational approaches, ribose-seq (Balachander et al., 2019) and Ribose-Map (Gombolay et al., 2019), allow for the efficient construction and analysis of genomic libraries derived from any DNA source containing rNMPs. Exploiting these techniques, we focused on the unicellular green alga of the species *Chlamydomonas reinhardtii*, which is broadly distributed worldwide in soil and freshwater. *C. reinhardtii* is used in production of biofuels (Sasso et al., 2018). It is also used to study photosynthesis and cell mobility (Sasso et al., 2018). We built ribose-seq libraries of rNMP incorporation from three independent cultures of *C. reinhardtii* cells grown in the light. We found a strongly biased frequency of incorporation of rAMP in the mitochondrial and chloroplast DNA, and we characterized the overall genomic rNMP distribution in these algal cells. Moreover, to characterize the capacity of *C. reinhardtii* to process rNMPs embedded in DNA, we identified genes and proteins of RNase H2 in the alga with help of the GeneMark-EP+ pipeline (Bruna et al., 2020).

## RESULTS

### ***C. reinhardtii* cells have a high ATP/dATP ratio**

With the goal to study the composition and distribution of rNMPs in the DNA of *C. reinhardtii* cells, we first determined the concentration of nucleotide triphosphates (NTPs) and dNTPs in these algal cells. *C. reinhardtii* (strain CC-1690) cells were grown in the light for 5–7 days to reach optical density (O.D.) = 1.5–1.7 at 750 nm corresponding to  $2 \times 10^6$  cells/mL. Cells were lysed, and cell extracts were prepared for mass spectrometry analyses of the NTP (ATP, CTP, GTP, and UTP) and dNTP (dATP, dCTP, dGTP, and dTTP) pools. The mass spectrometry analyses revealed strong abundance of ATP in the *C. reinhardtii* cells (Figure 1A). While NTPs are generally more abundant than dNTPs in cells, with NTP concentrations being one to three orders of magnitude higher than those of dNTPs (Clausen et al., 2013; Ferraro et al., 2010), a key factor contributing to misincorporation of rNMPs in DNA is a variation in nucleotide pool concentrations resulting in an increased NTP/dNTP ratio for one or more nucleotides (Ferraro et al., 2010; Wanrooij et al., 2017). In *C. reinhardtii* cells, the ATP/dATP ratio was by far the largest of the NTP/dNTP ratios in these cells (Figure 1B) and significantly higher than all other NTP/dNTP ratios (CTP/dCTP, GTP/dGTP, and UTP/dTTP,  $p = 0.0007$ ,  $0.004$ , and  $0.0006$ , respectively). Compared to the previously recorded ATP/dATP ratios obtained for yeast cells, varying from ~100 to ~300 in *S. cerevisiae* and ~750 in *S. pombe* (Balachander et al., 2020; Clausen et al., 2013) and between ~130 and ~350 in human dividing cells and ~1,450 in human non-dividing cells (Clausen et al., 2013; Ferraro et al., 2010; Traut, 1994), the ATP/dATP ratio that we measured in *C. reinhardtii* cells is the highest, ~1,800 (Figure 1B). To determine whether the high ATP/dATP ratio observed in *C. reinhardtii* cells was due to the exposure to the light during cell growth, we measured the NTP and dNTP concentrations from algal cells that were grown in the dark

A

Sample	Concentration of dNTPs and rNTPs: pmols per 10 <sup>7</sup> cells							
<i>C. reinhardtii</i>	rATP	rCTP	rGTP	rUTP	dATP	dCTP	dGTP	dTTP
1	76.8	8.91	18	7.36	0.041	BLOQ	0.047	BLOQ
2	51.5	6.04	15.1	5.38	0.021	BLOQ	0.057	0.063
3	86.1	10.2	20.1	7.8	0.063	0.011	0.082	0.032
4	68.2	6.71	17	5.85	0.044	0.011	0.058	0.039

B

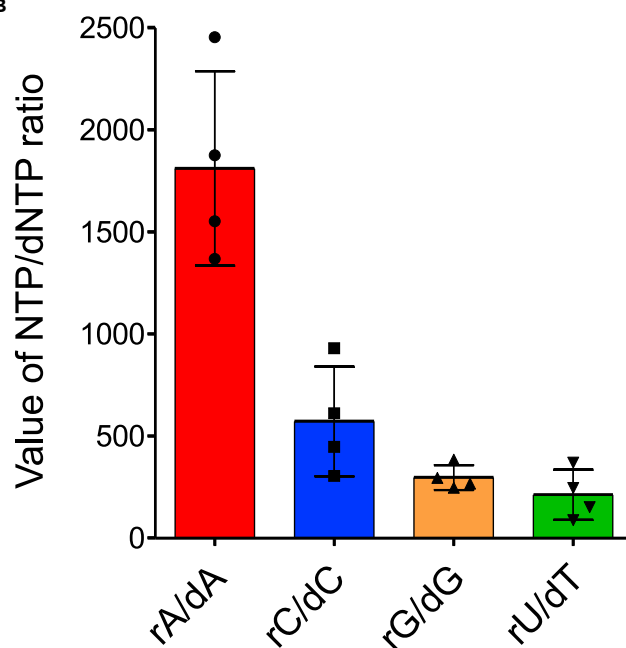


**Figure 1. Measurements of NTP and dNTP levels in *C. reinhardtii* cells show high ATP concentration**

(A) The levels of NTPs and dNTPs extracted from known numbers of algal cells of *C. reinhardtii* strain CC-1690 were determined by liquid chromatography with tandem mass spectrometry (LC-MS-MS) methods (see [Methods](#)). BLOQ: below limit of quantification. The cellular level of each nucleotide was normalized for 10<sup>7</sup> cells.

(B) The NTP and dNTP levels determined in (A) were used to calculate the NTP/dNTP ratios. Shown are mean and standard deviation of four repeats for each sample. Ratios for dCTP and dTTP levels below the limit of quantification were calculated by using the limit value of quantification for dCTP or dTTP (0.02 pmole) relative to the number of cells used in the LC-MS/MS method. The ratio of ATP/dATP was clearly significantly higher than all other NTP/dNTP (CTP/dCTP, GTP/dGTP, and UTP/dTTP) ratios,  $p = 0.0007$ ,  $0.004$ , and  $0.0006$ , respectively.

for 10–12 days to reach O.D. = 1.5–1.7 at 750 nm corresponding to  $2 \times 10^6$  cells/mL. While we found a slight decrease of the ATP/dATP ratio for cells grown in the dark, this ratio remained high and the largest compared to the other NTP/dNTP ratios ([Figure S1](#)). These results suggest that the high ATP/dATP ratio is a feature of the algal *C. reinhardtii* cells and it is independent from photosynthesis.

### Mitochondrial and chloroplast DNA of *C. reinhardtii* have overriding incorporation of rA

To determine the pattern of rNMPs in the mitochondrial, chloroplast, and nuclear genome of *C. reinhardtii* cells, we extracted the whole genomic DNA from three independent cultures of these cells grown in light (see [Transparent methods](#)). From these three DNA extracts, we constructed three genomic libraries using

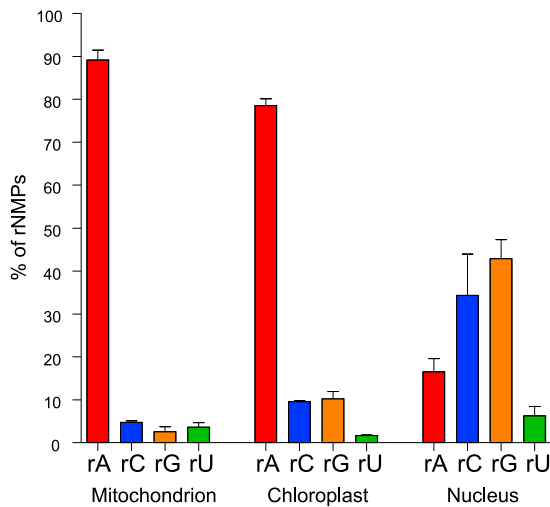


**Figure 2. High frequency of rA in mitochondrial and chloroplast but not nuclear genome of *C. reinhardtii* cells**

Bar graph with the percentage of rA, rC, rG, and rU found in mitochondrial, chloroplast, and nuclear DNA of *C. reinhardtii* cells. Mean and standard deviation from three different mitochondrial, chloroplast, or nuclear ribose-seq libraries are shown.

the ribose-seq approach (see [Transparent methods](#) and [Table S1](#)): FS121, FS231, and FS232 ([Table S2](#)). Each of these ribose-seq libraries was sequenced and then segmented into a mitochondrial, chloroplast, and nuclear library using the Ribose-Map computational toolkit after alignment of the sequencing reads to the reference genome sequence of *C. reinhardtii*. We obtained the mitochondrial and chloroplast sequences from the NCBI (<https://www.ncbi.nlm.nih.gov/genome/147>) and the 5.5 nuclear sequence from the Joint Genome Institute (JGI) ([https://phytozome.jgi.doe.gov/pz/portal.html#!info?alias=Org\\_Creinhardtii](https://phytozome.jgi.doe.gov/pz/portal.html#!info?alias=Org_Creinhardtii)). The percentage of rNMPs with base A, C, G and U (rA, rC, rG, and rU) varies strikingly between ribose-seq libraries of the organelles and nuclear DNA. Remarkably, both the mitochondrial and chloroplast DNA display a noticeable preference for rA with an average of 89% rA in mitochondrial and 77% rA in chloroplast DNA ([Figure 2](#) and [Table S2](#)). As shown by our analysis of the rNMP content in mitochondrial and chloroplast DNA of *C. reinhardtii* cells, rA is significantly and disproportionately incorporated relative to rC, rG, and rU and relative to the nucleotide content of these genomes ([Figures 3A–3D, 4A, and 5A](#) and [Tables S3](#) and [S3B](#)). The biased incorporation of rA in these organelles likely reflects the high ratio of ATP/dATP in the algal cells ([Figure 1B](#)). Interestingly, while rC, rG, and rU are all similarly infrequent in the mitochondrial DNA, rU is distinctly the least abundant rNMP in the chloroplast DNA, even if rC and rG are much less frequent than rA, as evidenced via nucleotide frequency and heatmap analyses ([Figures 3A–3D, 4A, and 5A, and Tables S3](#) and [S3B](#)). The rNMP composition found in mitochondrial and chloroplast DNA of *C. reinhardtii* is maintained similarly between the forward and reverse strands of these genomes ([Table S2](#)).

### Nuclear DNA of *C. reinhardtii* has higher level of rG and rC and lower level of rA and rU

The nuclear rNMPs were uniformly distributed across the nuclear genome with the percentage of rNMPs being proportional to the *C. reinhardtii* chromosome sizes ([Figure S2](#)). The composition of rNMPs in nuclear DNA showed more abundant rG and rC, followed by rA ([Figures 2, 3E, 3F, and 6A, and Table S2](#)). rU was consistently the least abundant rNMP in the nuclear DNA of the three libraries and on average a factor of ~2.8 and up to a factor of 4.7 below the nuclear-dT content ([Figures 3E, 3F, and 6A, and Tables S2](#) and [S3](#)). As for mitochondrial and chloroplast DNA, the rNMP composition found in nuclear DNA of *C. reinhardtii* is maintained similarly between the forward and reverse strands of these genomes ([Table S2](#)). Normalization of single rNMP frequencies to the nucleotide base content of *C. reinhardtii* nuclear DNA revealed rNMP incorporation with a marked preference for rG and/or rC in all the nuclear libraries over rA and especially over rU ([Figure 6A](#) and [Table S3](#)). These nuclear data do not reflect the nucleotide pool composition of *C. reinhardtii* cells because, as shown above, among the measured ratios of NTPs/dNTPs in the algal cells, the ATP/dATP is the highest one ([Figure 1B](#)). These results suggest possible active removal of rA from nuclear DNA but not from the mitochondrial and chloroplast genomes.

### Evaluation of RNase H2 activity in the algal cells and identification of the genes coding for the three subunits of RNase H2 in the *C. reinhardtii* genome

To examine whether the *C. reinhardtii* cells of strain CC-1690 displayed RNase H2 activity or other similar activity on a DNA substrate containing an embedded rNMP, protein extracts ([Figure S3](#)) were prepared to

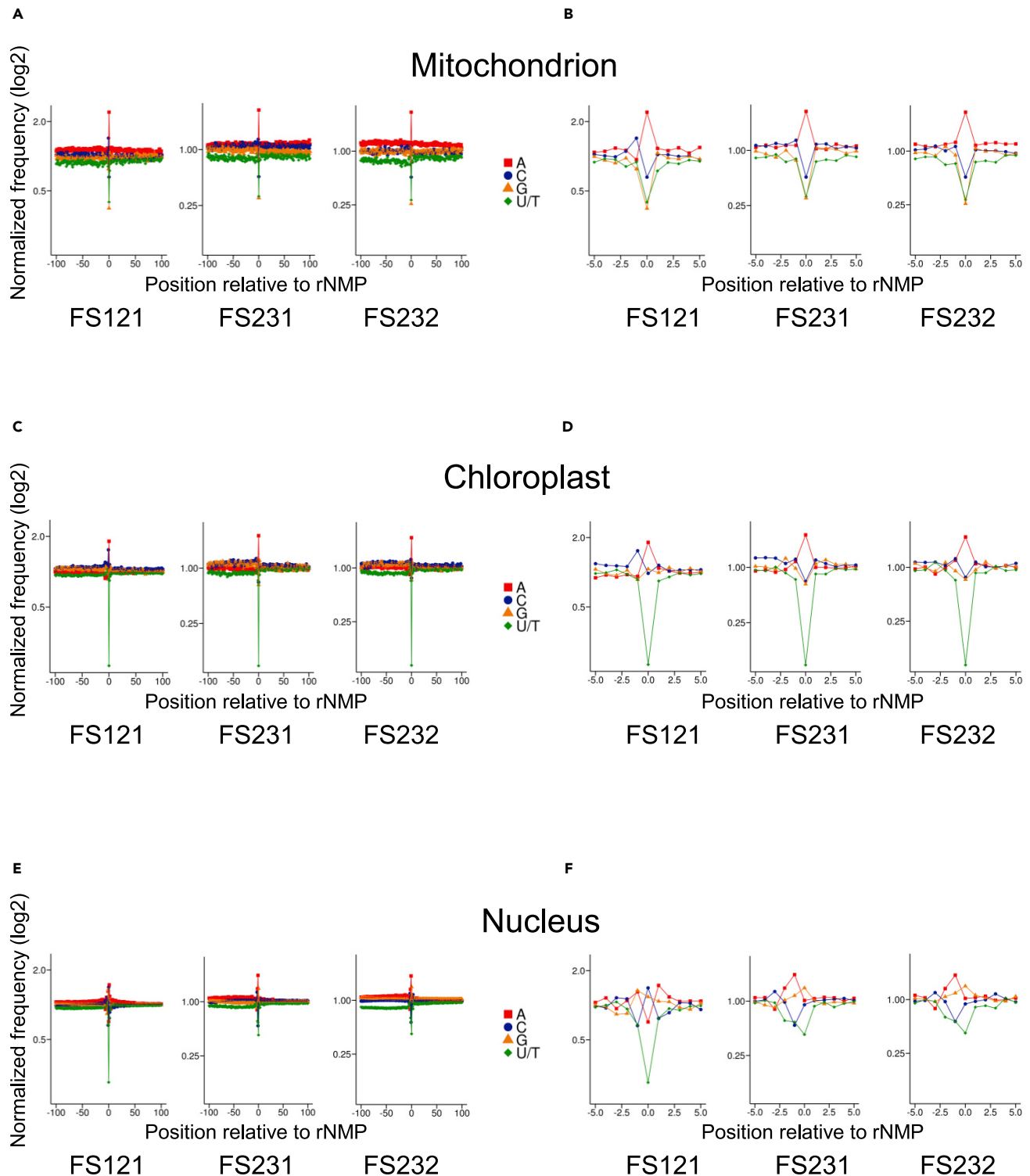


**Figure 3. Identity and sequence context of rNMPs in mitochondrial, chloroplast, and nuclear DNA of *C. reinhardtii* cells**

Zoomed out (A, C, and E) and zoomed in (B, D, and F) plots of normalized nucleotide frequencies relative to mapped positions of sequences from mitochondrial (A and B), chloroplast (C and D), and nuclear (E and F) ribose-seq libraries. Position 0 is the rNMP; - and + positions are upstream and downstream dNMPs, respectively, normalized to the A, C, G, and T content in the genome of *C. reinhardtii*. The y axis shows the frequency of each type of nucleotide present in the ribose-seq data normalized to the frequency of the corresponding nucleotide present in the reference genome of the indicated cell compartment of *C. reinhardtii*. Red square, A; blue circle, C; orange triangle, G; and green rhombus, U. Red square, A; blue circle, C; orange triangle, G; and green rhombus, U.

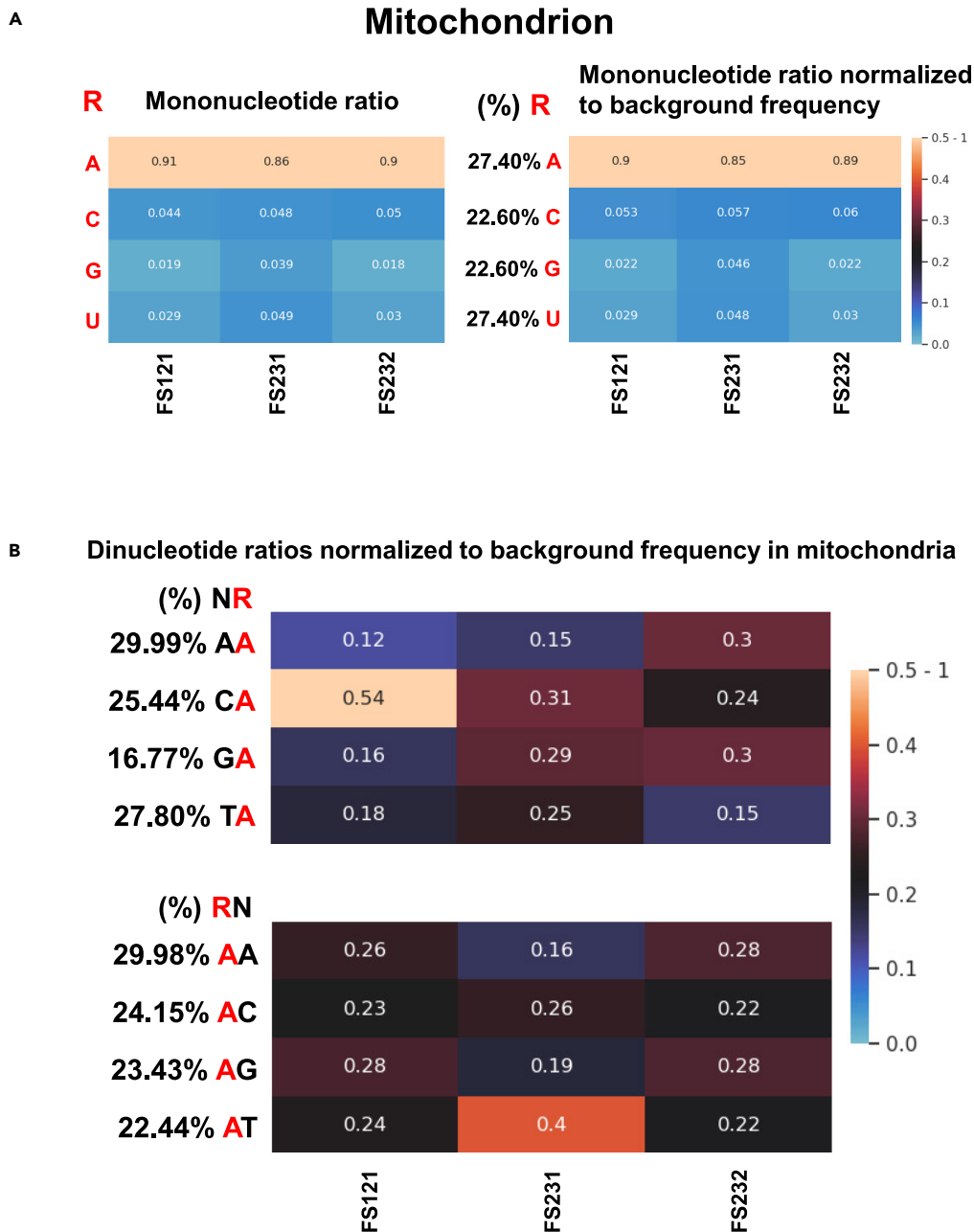


**Figure 4. rA is by large the most abundantly incorporated rNMP in *C. reinhardtii* mitochondrial DNA**

(A) Heatmap analyses with (left) ratio of each type of rNMP (rA, rC, rG, and rU) and (right) ratio of each type of rNMP normalized to the nucleotide frequencies of the *C. reinhardtii* mitochondrial reference genome for the mitochondrial ribose-seq libraries of this study. The corresponding formulas used are shown in (B) and explained in the [Transparent methods](#). Each column of the heatmap shows results of a specific ribose-seq library. Each library name is indicated underneath each column of the heatmap. Each row shows results obtained for an rNMP (R in red) of base A, C, G, or U for each library. The actual percentage of A, C, G, and T bases present in mitochondrial DNA of *C. reinhardtii* is shown to the left of the heatmap with normalized data. The bar to the right shows how different ratio values are represented as different colors. Black corresponds to 0.25.

(B) Heatmap analyses with normalized frequency of mitochondrial NR (top) and RN (bottom) dinucleotides containing rA with the upstream (top) or downstream (bottom) deoxyribonucleotide with base A, C, G, or T for the mitochondrial ribose-seq libraries of this study. The formulas used to calculate these normalized frequencies are shown and explained in the [Transparent methods](#). Each column of the heatmap shows results of a specific ribose-seq library. Each library name is indicated underneath each column of the heatmap. Each row shows results obtained for a dinucleotide NR or RN (R in red)

**Figure 4. Continued**

of fixed rNMP base A for each library. The actual percentage of dinucleotides of fixed base A for the indicated base combinations (AA, CA, GA, and TA, top; and AA, AC, AG, and AT, bottom) present in mitochondrial DNA of *C. reinhardtii* is shown to the left of the corresponding heatmaps. The observed percentage of dinucleotides with rA was divided by the actual percentage of each dinucleotide with fixed base A in mitochondrial DNA of *C. reinhardtii*. The bar to the right shows how different frequency values are represented as different colors. Black corresponds to 0.25. Significance of comparisons for data in this figure is shown in Table S3A.

examine their activity to cleave a substrate with one rG or one rA (see Transparent methods). Cleavage of these substrates by *E. coli* RNase HII was used as a positive control. The results show that *C. reinhardtii* protein extract is not active on an rG in DNA because the dsDNA substrate was not cleaved at the rNMP position (Figure S3). Similar results were obtained using the DNA substrate containing rA (Figure S3). No active cleavage of rNMP-containing substrates from the *C. reinhardtii* protein extract was detected. It is possible that the RNase H2 activity in *C. reinhardtii* cells is weak. At the same time, we cannot exclude the possibility that the protein extract is either missing some cofactor necessary for the RNase H2 function of *C. reinhardtii* or it may contain some inhibitory factor for RNase H2, preventing RNase H2 from cutting the rNMP-containing substrates. When we treated the substrate containing the rG with *E. coli* RNase HII both in the presence and the absence of the algal protein extract, we noticed a modest decrease of RNase HII cleavage activity in the presence of the algal protein extract, although cleavage at the rG was still efficient (Figure S3).

To identify genes for RNase H2 subunits A, B, and C in the genome of *C. reinhardtii*, we used gene finder GeneMark-EP+ (Bruna et al., 2020). For finding gene for the subunit A, it was sufficient to run a component of GeneMark-EP+, the protein mapping ProtHint pipeline that detected relationship between the RNase H2 subunit A family of proteins and a gene in the *C. reinhardtii* chromosome 17 in positions 754,797–758,398, encoding a protein apparently homologous to 915 out of 1,059 target RNase H2 subunit A proteins from other species. The gene corresponded to a hypothetical *C. reinhardtii* protein (PNW69996.1). Multiple sequence alignments of the primary structure of this protein with primary structures of RNase H2 subunit A proteins from *S. cerevisiae*, *Arabidopsis thaliana*, and *Homo sapiens* showed patterns of significant conservation (Figure 7). Pairwise similarity between the *C. reinhardtii* protein and each of the homologous proteins from the three species was statistically significant ( $E < 1 \times 10^{-45}$ ) when each of the three proteins was used as a query in the Protein Basic Local Alignment Search Tool (BLASTp) search against the *C. reinhardtii* proteome. Search for genes of RNase H2 subunits B and C was more complicated since these two subunits are less conserved among species related to the alga. In these cases, we had to make a full run of GeneMark-EP+ to re-predict genes in *C. reinhardtii* genome and, subsequently, to make a second iteration of ProtHint running in a more sensitive mode. As a result, the gene of subunit B was found in positions 1,174,994–1,176,998 in chromosome 7; this gene encoded a protein homologous to 373 out of 719 target RNase H2 subunit B proteins. The homologous gene of subunit C was found in positions 3,889,513–3,890,347 in chromosome 8; this gene encoded a protein homologous to 330 out of 662 target RNase H2 subunit C proteins (Figure 7). As a future direction, it will be interesting to target these potential RNase H2 genes to generate mutants and study how these affect the composition, distribution, and patterns of rNMP presence in the nuclear genome of *C. reinhardtii*.

**rA found in mitochondrial and chloroplast DNA and rC, rG, and rA found in nuclear DNA are non-uniformly distributed**

We then studied whether rA is uniformly distributed in the mitochondrial and chloroplast DNA of the three *C. reinhardtii* libraries. If, for example, rA is uniformly distributed in *C. reinhardtii* mitochondrial DNA, the frequency by which the dNMP with base A, C, G, or T is found at position -1 and +1 relative to rA should reflect the frequency of the dinucleotides AA, CA, GA, TA, AC, AG, and AT obtained from the sequence of *C. reinhardtii* mitochondrial DNA. The heatmap dinucleotide analysis revealed that the frequency of the dNMPs immediately upstream (at position -1) of the rAMP and in part the dNMP at position +1 and -3 from the rAMP in mitochondrial DNA deviates from the expected values but varies among the three mitochondrial libraries (Figures 4B and S4A and Table S3). Possibly, incorporation of rA in mitochondrial DNA may be more sensitive to small variations in growth conditions of the cells used to prepare the ribose-seq libraries analyzed in this study. No bias was found for the nucleotide upstream or downstream of the rAMP at positions -2, +2, +3, -4,+4, -5, +5, -6, +6, -100, and +100 in the mitochondrial DNA (Figure S4). In fact, with the increased gap between dinucleotide pairs (from -2, +2 to -6, +6 and -100 and +100), the uniformity is strengthened, as evidenced by an increased p-value from -1, +1 to -100



## Chloroplast

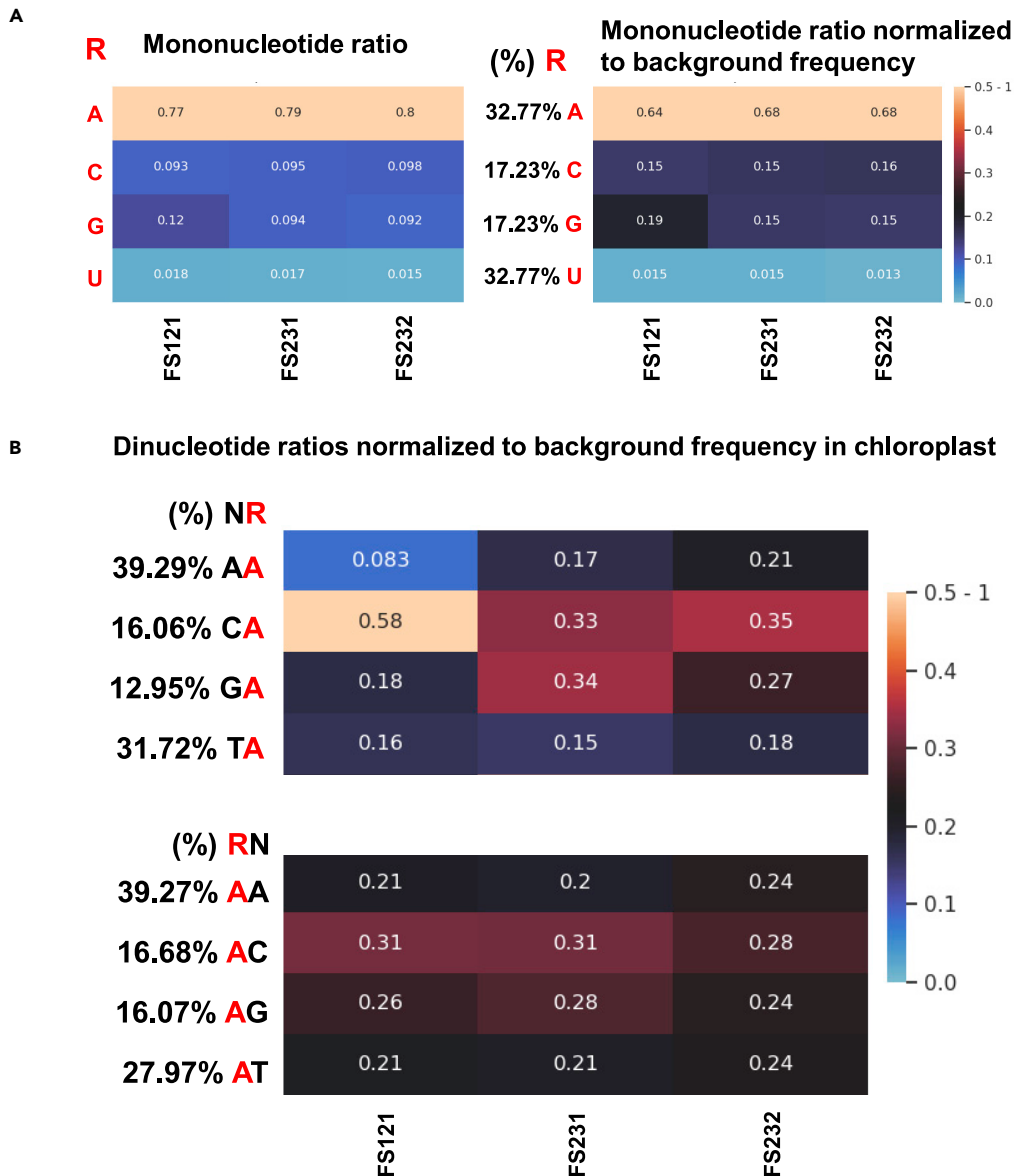


**Figure 5. rA is dominant and not uniformly distributed in *C. reinhardtii* chloroplast DNA**

(A) Heatmap analyses with (left) ratio of each type of rNMP (rA, rC, rG and rU) and (right) ratio of each type of rNMP normalized to the nucleotide frequencies of the *C. reinhardtii* chloroplast reference genome for the chloroplast ribose-seq libraries of this study. The corresponding formulas used are explained in the [Transparent methods](#). Each column of the heatmap shows results of a specific ribose-seq library. Each library name is indicated underneath each column of the heatmap. Each row shows results obtained for an rNMP (R in red) of base A, C, G, or U for each library. The actual percentage of A, C, G, and T bases present in chloroplast DNA of *C. reinhardtii* is shown to the left of the heatmap with normalized data. The bar to the right shows how different ratio values are represented as different colors. Black corresponds to 0.25.

(B) Heatmap analyses with normalized frequency of chloroplast NR (top) and RN (bottom) dinucleotides containing rA with the upstream (top) or downstream (bottom) deoxyribonucleotide with base A, C, G, or T for the chloroplast ribose-seq libraries of this study. The formulas used to calculate these normalized frequencies are shown and explained in the [Transparent methods](#). Each column of the heatmap shows results of a specific ribose-seq library. Each library name is indicated underneath each column of the heatmap. Each row shows results obtained for a dinucleotide NR or RN (R in red) of fixed rNMP base A for each library. The actual percentage of dinucleotides of fixed base A for the indicated base

**Figure 5. Continued**

combinations (AA, CA, GA, and TA, top; and AA, AC, AG, and AT, bottom) present in chloroplast DNA of *C. reinhardtii* is shown to the left of the corresponding heatmaps. The observed percentage of dinucleotides with rA was divided by the actual percentage of each dinucleotide with fixed base A in chloroplast DNA of *C. reinhardtii*. The bar to the right shows how different frequency values are represented as different colors. Black corresponds to 0.25. Significance of comparisons for data in this figure is shown in Table S3B.

and +100 (Table S3). For the chloroplast DNA, the rAMP was preferentially found downstream of dC and more rarely downstream of dA and dT (Figure 5B and Table S3). No particular bias was found for the nucleotide upstream or downstream of the rAMP at positions +1, -2, +2, -3, +3, -4,+4, -5, +5, -6, +6, -100, and +100 in the chloroplast DNA (Figure S4 and Table S3). Due to the low abundance of rC, rG, and rU in the mitochondrial and chloroplast DNA, we did not analyze the surrounding dNMPs of these rNMPs.

For nuclear DNA, we found that both rC and rG are preferentially preceded by dA at position -1. The observed count of NR dinucleotides with an rC or rG (dArC, dCrC, dGrC, and dTrC; dArG, dCrG, dGrG, and dTrG) was significantly different from the expected count calculated for the background frequency of the corresponding dinucleotide pair with the same number of total rCMPs or rGMPs (Table S3). The observed count of the dinucleotide dArC was above the expected count for this pair (Figure 6B and Table S3). Similarly, the observed count of dArG was above the expected count for this pair (Figure 6B and Table S3). For rA, we found that the dArA count was above the expected count for this dinucleotide in all libraries, while for rU, the pattern was less clear, possibly due to the fact that rU is the least abundant rNMP found in the nuclear DNA of *C. reinhardtii* cells, and more data would be needed to obtain an accurate spectrum of incorporation (Figure 6B and Table S3). A much less prominent difference was found among pair combinations for the dNMPs at position +1 (Figure 6B and Table S3). We also examined the dNMPs at positions -2, +2, -3, +3, -4,+4, -5, +5, -6, +6, -100, and +100. The heatmaps progressively became uniformly darker from -2, +2 to -100, +100, while no particular pattern emerging (Figure S5 and Table S3C). Overall, these results, which were also conserved among all three nuclear libraries, highlight the fact that the dNMPs immediately upstream of the rNMP at position -1 have the most impact on the incorporation of a specific rNMP type in a given genomic position of the algal nuclear DNA. Moreover, these findings demonstrate that rNMPs are not randomly incorporated in the nuclear genome of *C. reinhardtii* cells.

**DISCUSSION**

We report a genome-wide analysis of rNMP sites in a photosynthetic organism, the unicellular freshwater green alga *C. reinhardtii*. We found rNMPs embedded in all genomes of the alga: mitochondrial, chloroplast, and nuclear. We revealed strikingly biased rA incorporation in the mitochondrial and chloroplast DNA but not in the nuclear DNA, in which instead rG and rC are dominant over rA and rU. To our knowledge, there is no previously available report showing that DNA polymerases of *C. reinhardtii* are prone to incorporate rAMPs in genomic DNA of the alga. *C. reinhardtii*, like most non-opisthokonts (photosynthetic eukaryotes and protists), does not use DNA polymerase  $\gamma$  in the organelles, like animals and fungi, but the plant and protist organellar DNA polymerase (Moriyama et al., 2011). The disproportionate presence of rA embedded in the mitochondrial and chloroplast DNA reflects the remarkably high ATP/dATP ratio of the cells. These findings support the lack of RNase H2 activity in mitochondrial DNA and provide new evidence for the absence of RNase H2 activity on rNMPs embedded in chloroplast DNA. The inability to cleave and initiate removal of rNMPs embedded in mitochondrial and chloroplast DNA likely allows abundant incorporation of rNMPs in these genomes, particularly rA, significantly and markedly above the frequency expected based on the dA content of the mitochondrial and chloroplast genomes. Work in yeast cells has provided supportive evidence for a frequent exchange of nuclear and mitochondrial dNTP pools (Wanrooij et al., 2017). Thus, although there is no direct proof that this occurs in *C. reinhardtii* cells, we would expect rA to also be highly incorporated in the nuclear genome of *C. reinhardtii*. Because rA was not found to be the most frequently incorporated rNMP in the nuclear DNA of *C. reinhardtii*, but rather rG and rC were more frequently detected, our findings suggest that RNase H2 might have a high workload in removing rA from the nuclear genome of a photosynthetic organism, such as *C. reinhardtii*. Nevertheless, we were unable to detect an RNase H2 or any other cleavage function from protein extracts of the algal cells to support active removal of rA from nuclear DNA. On the contrary, we were able to find hypothetical *C. reinhardtii* orthologous genes and proteins for RNase H2A, H2B, and H2C (Figure 7), suggesting that RNase H2 is present and likely functional on rNMPs embedded in *C. reinhardtii* nuclear DNA. Knowing the position of the hypothetical RNase H2A, H2B, and H2C genes will help to design mutants in these

## Nucleus

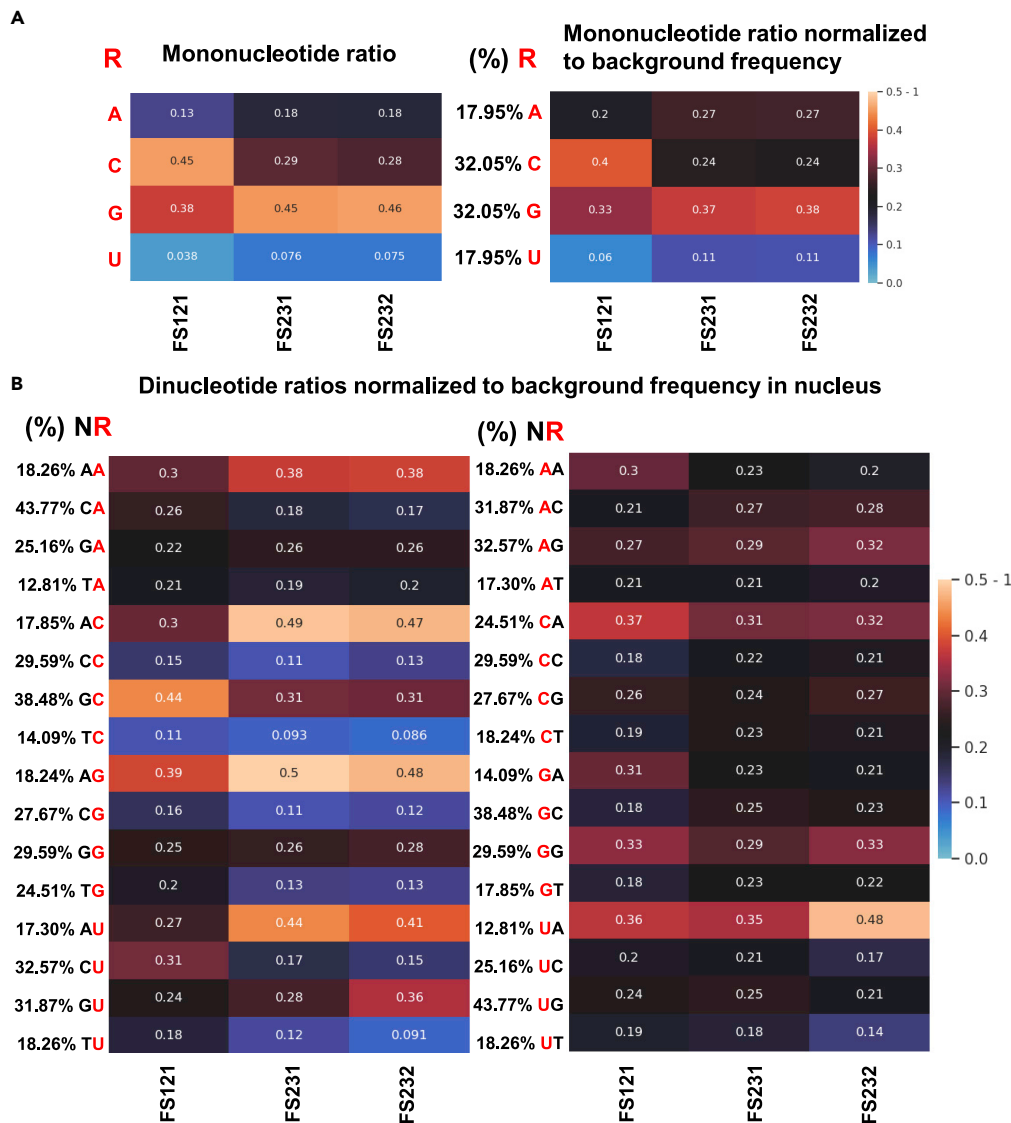


**Figure 6. rC and rG are dominant and not uniformly distributed in nuclear DNA of *C. reinhardtii* cells**

(A) Heatmap analyses with (left) ratio of each type of rNMP (rA, rC, rG, and rU) and (right) ratio of each type of rNMP normalized to the nucleotide frequencies of the *C. reinhardtii* nuclear reference genome for the nuclear ribose-seq libraries of this study. The corresponding formulas used are shown in the [Transparent methods](#). Each column of the heatmap shows results of a specific ribose-seq library. Each library name is indicated underneath each column of the heatmap. Each row shows results obtained for an rNMP (R in red) of base A, C, G, or U for each library. The actual percentage of A, C, G, and T bases present in nuclear DNA of *C. reinhardtii* is shown to the left of the heatmap with normalized data. The bar to the right shows how different ratio values are represented as different colors. Black corresponds to 0.25.

(B) Heatmap analyses with normalized frequency of nuclear NR (top) and RN (bottom) dinucleotides with rA, rC, rG, and rU with the upstream (left) or downstream (right) deoxyribonucleotide with base A, C, G, or T for the nuclear ribose-seq libraries of this study. The formulas used to calculate these normalized frequencies are shown and explained in the [Transparent methods](#). Each column of the heatmap shows results of a specific ribose-seq library. Each library name is indicated underneath each column of the heatmap. Each row shows results obtained for a dinucleotide NR or RN (R in red) of fixed base A, C, G, or T for the indicated base combinations for each library. The actual percentage of dinucleotides of fixed base A, C, G, or T present in nuclear DNA of *C. reinhardtii* is shown to the left of the corresponding heatmaps. The observed percentage of dinucleotides with rNMPs with base A, C, G, or U was divided by the actual percentage of each dinucleotide with fixed base A, C, G, or T in nuclear DNA of *C. reinhardtii*. The bar to the right shows how different frequency values are represented as different colors. Black corresponds to 0.25. Significance of comparisons for data in this figure is shown in [Table S3C](#).

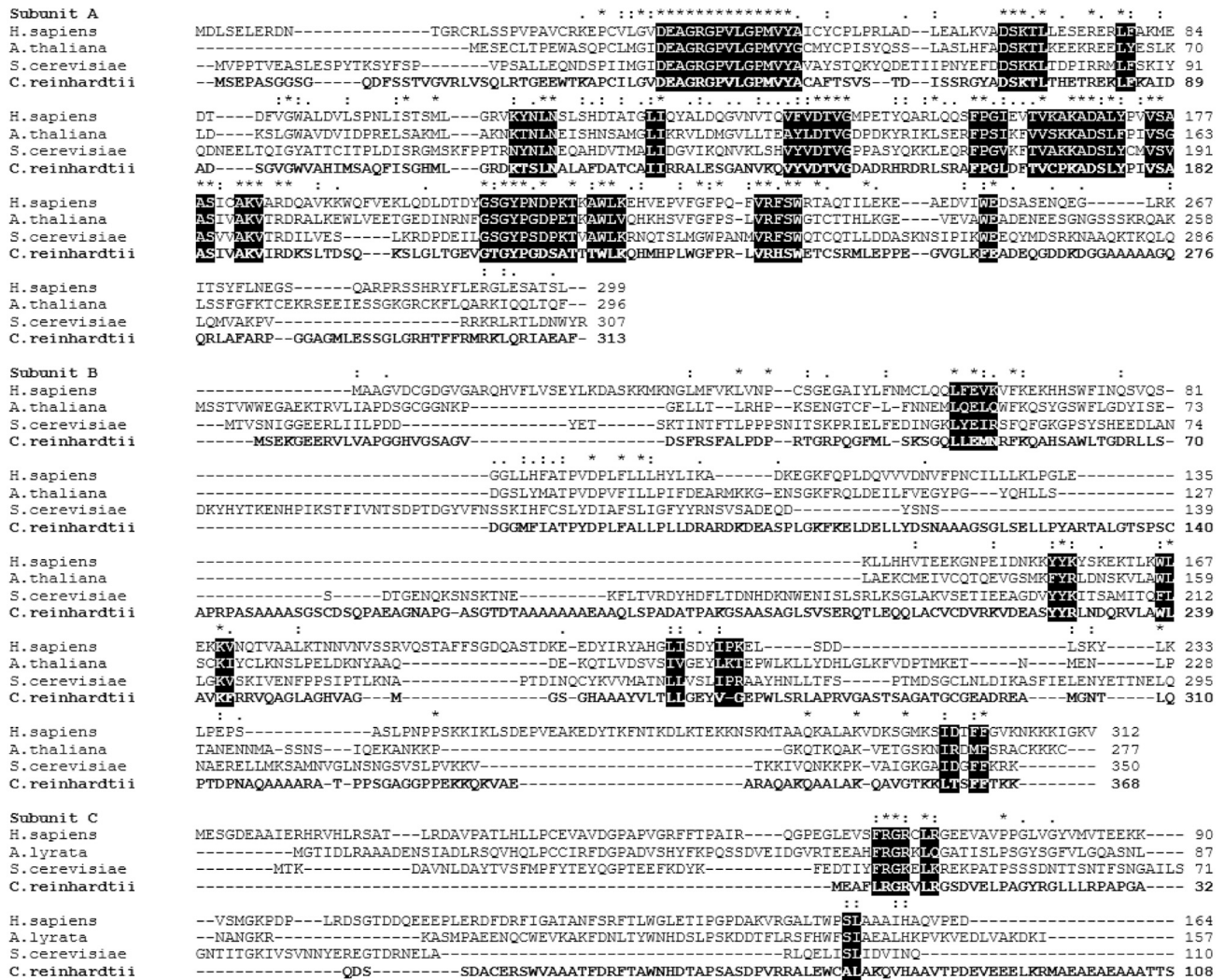


**Figure 7. Hypothetical RNase H2 proteins of *C. reinhardtii***

Multiple alignment of amino acid sequences of RNase H2 catalytic subunit H2A, and accessory subunits H2B and H2C from *H. sapiens*, *S. cerevisiae*, *A. thaliana* (*A. lyrata* for subunit C) (Cerritelli and Crouch, 2009) (Kalhorzadeh et al., 2014) and the hypothetical proteins of *C. reinhardtii*. The *C. reinhardtii* hypothetical proteins are shown in bold. The highlighted letters show the most conserved parts of the four sequences.

loci to study how defects in RNase H2 genes affect the profile of rNMPs in the nuclear, mitochondrial, and chloroplast genome of the alga. Moreover, it will be valuable to work with a purified RNase H2 enzyme from *C. reinhardtii* cells to characterize its activity on rNMPs embedded in DNA. There is also the possibility that the nuclear DNA polymerases of *C. reinhardtii* have a much stronger discrimination capacity for ATP vs. dATP than the DNA polymerases of the mitochondria and chloroplast of the alga. Further studies are needed to understand how rA is specifically excluded from the nuclear DNA of *C. reinhardtii* cells. In addition, it would also be interesting to investigate the relation between rNMP incorporation in the mitochondrial and chloroplast DNA of the alga and the process of photosynthesis.

If we compare the rNMP content in the mitochondrial DNA of *C. reinhardtii* with that of *S. cerevisiae*, *S. paradoxus*, and *S. pombe*, we find that rU is the least incorporated rNMP not only in mitochondrial and chloroplast DNA of the alga, as in the yeast mitochondria, but also in nuclear DNA of the alga. Differently, in yeast nuclear DNA, rU is the least frequent rNMP only in RNase H2-defective cells (Balachander et al., 2020). In part, the low level of rU incorporation could reflect the relatively low UTP/dTTP ratio in these eukaryotic cells. Activity of topoisomerase I on sequences with rU (Cho and Jinks-Robertson, 2018; Klein,

2017) and some proofreading activity for nuclear DNA polymerase on rU (Koh et al., 2015) could contribute to the general rare presence of rU in these genomes. Moreover, in each of the three yeast species, rA is incorporated significantly below the expected values (0.25) for the corresponding genomes. Instead, rC and rG are the predominant rNMPs (Balachander et al., 2020). Our results show that the high ATP/dATP ratio in *C. reinhardtii* cells reflects the composition of rNMPs in the mitochondrial and chloroplast DNA of *C. reinhardtii*. Interestingly, rA incorporation was found mainly downstream of dC and/or dG in chloroplast DNA. However, no conserved pattern around rA was found in the mitochondrial DNA of all the three ribose-seq libraries of *C. reinhardtii*. At the same time, rA did display a library-specific preference of incorporation downstream of specific dNMPs in the mitochondrial DNA. It is possible that small variations in growth conditions may affect the incorporation pattern of rA in the algal mitochondrial DNA. While rU is consistently the least represented rNMP in the nuclear, mitochondrial, and chloroplast DNA of *C. reinhardtii* cells, the mitochondrial DNA also showed very low rG and rC content. Despite highly abundant rA incorporation is a common feature in the mitochondrial and chloroplast DNA of *C. reinhardtii*, the overall patterns of rNMP incorporation in these two algal organelles are not identical. These results suggest that the two organelles may have different rNMP incorporation mechanisms and/or that the composition of the nucleotide pools in these two organelles is different.

Another conserved feature between yeast and *C. reinhardtii* rNMP patterns, particularly for the nuclear DNA of the alga, is that the dNMP immediately upstream from the rNMP is the one that has the largest impact on the distribution of rNMPs. In fact, with the increased gap between dinucleotide pairs with an rNMP (from -1, +1 to -100, +100), the uniformity is strengthened not only for nuclear rNMPs but also for the mitochondrial and chloroplast rNMPs, as shown by increased p-value from -1, +1 dinucleotides to -100 and +100 dinucleotides (Tables S3A–S3C). Similarly to what we found for rNMPs in the yeast genome (Balachander et al., 2020), we believe that this biased presence of rNMPs in the algal genome supports an accommodation mechanism by DNA polymerases that facilitates incorporation of rNMPs following specific dNMPs.

In conclusion, via mapping and genome-wide analysis of ribose-seq libraries of the unicellular green alga *C. reinhardtii*, we have revealed a unique distribution of rNMPs embedded in the DNA of the algal organelles compared to the nuclear DNA of the same cells. It will be interesting to characterize how such disproportionate presence of rA in the genome of the organelles of this photosynthetic organism impacts the DNA metabolic functions of these genomes during their day and night cycles.

### Limitations of the study

In this study, we could not prove the activity of the RNase H2 enzyme from *C. reinhardtii* on rNMP-containing substrates *in vitro*. Thus, while our data strongly support the presence of a functional RNase H2 enzyme to cleave at rNMPs embedded in the nuclear DNA of *C. reinhardtii*, we do not provide direct proof of such function. Nonetheless, we have identified the potential genes for the three subunits of RNase H2 in *C. reinhardtii*. Therefore, we have set the stage for mutation experiments in these genes, to examine the activity of RNase H2 on rNMPs incorporated in the genome of *C. reinhardtii* cells.

### Resource availability

#### Lead contact

Further information and requests for resources and reagents should be directed to and will be fulfilled by the Lead Contact, Francesca Storici ([storici@gatech.edu](mailto:storici@gatech.edu)).

#### Materials Availability

All unique/stable reagents generated in this study are available from the Lead contact.

#### Data and Code Availability

The authors declare that the data supporting the findings of this study are available within the paper and its supplementary information files. The Ribose-Map bioinformatics toolkit is available for download at GitHub (<https://github.com/agombolay/ribose-map>). See also (Gombolay et al., 2019). Custom Python3 scripts for background subtraction is available for download at GitHub under GNU GPL v3.0 license (<https://github.com/xph9876/ArtificialRiboseDetection>). The custom Python3 scripts for heatmaps is available for download at GitHub under GNU GPL v3.0 license (<https://github.com/xph9876/RibosePreferenceAnalysis>) Table S2 contains raw data. Bar graphs representing the percentage of each

type of rNMP were made using GraphPad Prism 5 (GraphPad Software). The nucleotide sequence context plots were created using custom R scripts. The datasets generated during this study are available at NCBI's SRA under BioProject ID PRJNA657931. All data generated in this study are available from the Lead contact.

## METHODS

All methods can be found in the accompanying [Transparent Methods supplemental file](#).

## SUPPLEMENTAL INFORMATION

Supplemental Information can be found online at <https://doi.org/10.1016/j.isci.2020.102005>.

## ACKNOWLEDGMENTS

We thank the Molecular Evolution Core with A. Bryksin at the Parker H. Petit Institute for Bioengineering and Bioscience of the Georgia Institute of Technology for high throughput sequencing, M.D. Herron and C. Lindsey for supplemental aliquots of *C. reinhardtii* CC-1690 cells, J. Choi for bioinformatics support, K. Mukherjee and D. Kundnani for critically reading the manuscript, and all members of the Storici laboratory for assistance and feedback on this study. We acknowledge funding from the Egyptian Cultural Affairs & Missions Sector, Cairo, Egypt (to W.M.M.E.), R01GM128145 (to M.B.), AI136581 (to B.K.), AI150451 (to B.K.), MH116695 (to R.F.S.), the National Institutes of Health (R01ES026243 to F.S.), and the Howard Hughes Medical Institute (Faculty Scholar grant 55108574 to F.S.) for supporting this work.

## AUTHOR CONTRIBUTIONS

Conceptualization, F.S. and W.M.M.E.; Methodology, W.M.M.E., A.L.G., P.X., T.Y., Y.J., S.B., G.N., S.T., N.E.B, T.B., M.B., Y.C., and F.S.; Investigation, W.M.M.E., A.L.G., P.X., T.Y., Y.J., S.B., and F.S.; Writing – Original Draft F.S.; Writing – Review & Editing W.M.M.E., A.L.G., P.X., T.Y., Y.J., S.B., G.N., M.B., B.K., and F.S.; Funding acquisition, M.B., R.F.S., B.K., and F.S.; Resources, M.B., R.F.S., B.K., Y.C., and F.S. All authors commented on and approved the manuscript.

## DECLARATION OF INTERESTS

We have a patent related to this study: Storici, F., Hesselberth, J.R., and Koh, K. D. Methods to detect ribonucleotides in deoxyribonucleic acids. U.S. Patent U.S. 10,787,703 B1 Sep. 29, 2020.

Received: August 24, 2020

Revised: November 29, 2020

Accepted: December 23, 2020

Published: January 22, 2021

## REFERENCES

- Astatke, M., Ng, K., Grindley, N.D., and Joyce, C.M. (1998). A single side chain prevents *Escherichia coli* DNA polymerase I (Klenow fragment) from incorporating ribonucleotides. *Proc. Natl. Acad. Sci. U S A* 95, 3402–3407.
- Balachander, S., Gombolay, A.L., Yang, T., Xu, P., Newnam, G., Keskin, H., El-Sayed, W.M.M., Bryksin, A.V., Tao, S., Bowen, N.E., et al. (2020). Ribonucleotide incorporation in yeast genomic DNA shows preference for cytosine and guanosine preceded by deoxyadenosine. *Nat. Commun.* 11, 2447.
- Balachander, S., Yang, T., Newnam, G., El-Sayed, W.M.M., Koh, K.D., and Storici, F. (2019). Capture of ribonucleotides in yeast genomic DNA using ribose-seq. *Methods Mol. Biol.* 2049, 17–37.
- Berglund, A.K., Navarrete, C., Engqvist, M.K., Hoberg, E., Szilagyi, Z., Taylor, R.W., Gustafsson, C.M., Falkenberg, M., and Clausen, A.R. (2017). Nucleotide pools dictate the identity and frequency of ribonucleotide incorporation in mitochondrial DNA. *PLoS Genet.* 13, e1006628.
- Bonnin, A., Lazaro, J.M., Blanco, L., and Salas, M. (1999). A single tyrosine prevents insertion of ribonucleotides in the eukaryotic-type phi29 DNA polymerase. *J. Mol. Biol.* 290, 241–251.
- Brown, J.A., and Suo, Z. (2011). Unlocking the sugar “steric gate” of DNA polymerases. *Biochemistry* 50, 1135–1142.
- Bruna, T., Lomsadze, A., and Borodovsky, M. (2020). GeneMark-EP+: eukaryotic gene prediction with self-training in the space of genes and proteins. *NAR Genom. Bioinform.* 2, lqaa026.
- Caldecott, K.W. (2014). Molecular biology. Ribose—an internal threat to DNA. *Science* 343, 260–261.
- Cavanaugh, N.A., Beard, W.A., and Wilson, S.H. (2010). DNA polymerase beta ribonucleotide discrimination: insertion, misinsertion, extension, and coding. *J. Biol. Chem.* 285, 24457–24465.
- Cerritelli, S.M., and Crouch, R.J. (2009). Ribonuclease H: the enzymes in eukaryotes. *FEBS J.* 276, 1494–1505.
- Chiu, H.C., Koh, K.D., Evich, M., Lesiak, A.L., Germann, M.W., Bongiorno, A., Riedo, E., and Storici, F. (2014). RNA intrusions change DNA elastic properties and structure. *Nanoscale* 6, 10009–10017.
- Cho, J.E., and Jinks-Robertson, S. (2018). Topoisomerase I and genome stability: the good and the bad. *Methods Mol. Biol.* 1703, 21–45.
- Clausen, A.R., Lujan, S.A., Burkholder, A.B., Orebaugh, C.D., Williams, J.S., Clausen, M.F., Malc, E.P., Mieczkowski, P.A., Fargo, D.C., Smith, D.J., et al. (2015). Tracking replication enzymology in vivo by genome-wide mapping of

- ribonucleotide incorporation. *Nat. Struct. Mol. Biol.* 22, 185–191.
- Clausen, A.R., Zhang, S., Burgers, P.M., Lee, M.Y., and Kunkel, T.A. (2013). Ribonucleotide incorporation, proofreading and bypass by human DNA polymerase delta. *DNA Repair (Amst)* 12, 121–127.
- Daigaku, Y., Keszthelyi, A., Müller, C.A., Miyabe, I., Brooks, T., Retkute, R., Hubank, M., Nieduszynski, C.A., and Carr, A.M. (2015). A global profile of replicative polymerase usage. *Nat. Struct. Mol. Biol.* 22, 192–198.
- Ferraro, P., Franzolin, E., Pontarin, G., Reichard, P., and Bianchi, V. (2010). Quantitation of cellular deoxynucleoside triphosphates. *Nucleic Acids Res.* 38, e85.
- Gombolay, A.L., Vannberg, F.O., and Storici, F. (2019). Ribose-Map: a bioinformatics toolkit to map ribonucleotides embedded in genomic DNA. *Nucleic Acids Res.* 47, e5.
- Gong, C., Bongiorno, P., Martins, A., Stephanou, N.C., Zhu, H., Shuman, S., and Glickman, M.S. (2005). Mechanism of nonhomologous end-joining in mycobacteria: a low-fidelity repair system driven by Ku, ligase D and ligase C. *Nat. Struct. Mol. Biol.* 12, 304–312.
- Gosavi, R.A., Moon, A.F., Kunkel, T.A., Pedersen, L.C., and Bebenek, K. (2012). The catalytic cycle for ribonucleotide incorporation by human DNA Pol lambda. *Nucleic Acids Res.* 40, 7518–7527.
- Grossman, L.I., Watson, R., and Vinograd, J. (1973). The presence of ribonucleotides in mature closed-circular mitochondrial DNA. *Proc. Natl. Acad. Sci. U S A* 70, 3339–3343.
- Jinks-Robertson, S., and Klein, H.L. (2015). Ribonucleotides in DNA: hidden in plain sight. *Nat. Struct. Mol. Biol.* 22, 176–178.
- Kalhorzadeh, P., Hu, Z., Cools, T., Amiard, S., Willing, E.M., De Winne, N., Gevaert, K., De Jaeger, G., Schneeberger, K., White, C.I., et al. (2014). Arabidopsis thaliana RNase H2 deficiency counteracts the needs for the WEE1 checkpoint kinase but triggers genome instability. *Plant Cell* 26, 3680–3692.
- Kasiviswanathan, R., and Copeland, W.C. (2011). Ribonucleotide discrimination and reverse transcription by the human mitochondrial DNA polymerase. *J. Biol. Chem.* 286, 31490–31500.
- Kennedy, E.M., Amie, S.M., Bambara, R.A., and Kim, B. (2012). Frequent incorporation of ribonucleotides during HIV-1 reverse transcription and their attenuated repair in macrophages. *J. Biol. Chem.* 287, 14280–14288.
- Klein, H.L. (2017). Genome instabilities arising from ribonucleotides in DNA. *DNA Repair (Amst)* 56, 26–32.
- Koh, K.D., Balachander, S., Hesselberth, J.R., and Storici, F. (2015). Ribose-seq: global mapping of ribonucleotides embedded in genomic DNA. *Nat. Methods* 12, 251–257.
- Kolodner, R., Warner, R.C., and Tewari, K.K. (1975). The presence of covalently linked ribonucleotides in the closed circular deoxyribonucleic acid from higher plants. *J. Biol. Chem.* 250, 7020–7026.
- Lemor, M., Kong, Z., Henry, E., Brizard, R., Laurent, S., Bosse, A., and Henneke, G. (2018). Differential activities of DNA polymerases in processing ribonucleotides during DNA synthesis in archaea. *J. Mol. Biol.* 430, 4908–4924.
- McDonald, J.P., Vaisman, A., Kuban, W., Goodman, M.F., and Woodgate, R. (2012). Mechanisms employed by *Escherichia coli* to prevent ribonucleotide incorporation into genomic DNA by pol V. *PLoS Genet.* 8, e1003030.
- Moon, A.F., Pryor, J.M., Ramsden, D.A., Kunkel, T.A., Bebenek, K., and Pedersen, L.C. (2017). Structural accommodation of ribonucleotide incorporation by the DNA repair enzyme polymerase Mu. *Nucleic Acids Res.* 45, 9138–9148.
- Moriyama, T., Terasawa, K., and Sato, N. (2011). Conservation of POPs, the plant organellar DNA polymerases, in eukaryotes. *Protist* 162, 177–187.
- Nava, G.M., Grasso, L., Sertic, S., Pellicoli, A., Muzi Falconi, M., and Lazzaro, F. (2020). One, No one, and one hundred thousand: the many forms of ribonucleotides in DNA. *Int. J. Mol. Sci.* 21, 1706.
- Nick McElhinny, S.A., and Ramsden, D.A. (2003). Polymerase mu is a DNA-directed DNA/RNA polymerase. *Mol. Cell Biol.* 23, 2309–2315.
- Nick McElhinny, S.A., Watts, B.E., Kumar, D., Watt, D.L., Lundstrom, E.B., Burgers, P.M., Johansson, E., Chabes, A., and Kunkel, T.A. (2010). Abundant ribonucleotide incorporation into DNA by yeast replicative polymerases. *Proc. Natl. Acad. Sci. U S A* 107, 4949–4954.
- Patel, P.H., and Loeb, L.A. (2000). Multiple amino acid substitutions allow DNA polymerases to synthesize RNA. *J. Biol. Chem.* 275, 40266–40272.
- Potenski, C.J., and Klein, H.L. (2014). How the misincorporation of ribonucleotides into genomic DNA can be both harmful and helpful to cells. *Nucleic Acids Res.* 42, 10226–10234.
- Reijns, M.A.M., Kemp, H., Ding, J., Marion de Procé, S., Jackson, A.P., and Taylor, M.S. (2015). Lagging strand replication shapes the mutational landscape of the genome. *Nature* 518, 502–506.
- Sasso, S., Stibor, H., Mittag, M., and Grossman, A.R. (2018). From molecular manipulation of domesticated *Chlamydomonas reinhardtii* to survival in nature. *Elife* 7, 39233.
- Sparks, J.L., Chon, H., Cerritelli, S.M., Kunkel, T.A., Johansson, E., Crouch, R.J., and Burgers, P.M. (2012). RNase H2-initiated ribonucleotide excision repair. *Mol. Cell* 47, 980–986.
- Traut, T.W. (1994). Physiological concentrations of purines and pyrimidines. *Mol. Cell. Biochem.* 140, 1–22.
- Vengrova, S., and Dalgaard, J.Z. (2006). The wild-type *Schizosaccharomyces pombe* mat1 imprint consists of two ribonucleotides. *EMBO Rep.* 7, 59–65.
- Wanrooij, P.H., Engqvist, M.K.M., Forslund, J.M.E., Navarrete, C., Nilsson, A.K., Sedman, J., Wanrooij, S., Clausen, A.R., and Chabes, A. (2017). Ribonucleotides incorporated by the yeast mitochondrial DNA polymerase are not repaired. *Proc. Natl. Acad. Sci. U S A* 114, 12466–12471.
- Williams, J.S., and Kunkel, T.A. (2014). Ribonucleotides in DNA: origins, repair and consequences. *DNA Repair (Amst)* 19, 27–37.
- Williams, J.S., Lujan, S.A., and Kunkel, T.A. (2016). Processing ribonucleotides incorporated during eukaryotic DNA replication. *Nat. Rev. Mol. Cell Biol.* 17, 350.
- Zhu, H., and Shuman, S. (2008). Bacterial nonhomologous end joining ligases preferentially seal breaks with a 3'-OH monoribonucleotide. *J. Biol. Chem.* 283, 8331–8339.

## Supplemental Information

**Disproportionate presence of adenosine**

**in mitochondrial and chloroplast**

**DNA of *Chlamydomonas reinhardtii***

**Waleed M.M. El-Sayed, Alli L. Gombolay, Penghao Xu, Taehwan Yang, Youngkyu Jeon, Sathya Balachander, Gary Newnam, Sijia Tao, Nicole E. Bowen, Tomáš Brůna, Mark Borodovsky, Raymond F. Schinazi, Baek Kim, Yongsheng Chen, and Francesca Storici**



iScience, Volume --

## **Supplemental Information**

### **Disproportionate presence of adenosine in mitochondrial and chloroplast DNA of *Chlamydomonas reinhardtii***

**Waleed M.M. El-Sayed, Alli L. Gombolay, Penghao Xu, Taehwan Yang, Youngkyu Jeon, Sathya Balachander, Gary Newnam, Sijia Tao, Nicole E. Bowen, Tomáš Brůna, Mark Borodovsky, Raymond F. Schinazi, Baek Kim, Yongsheng Chen, and Francesca Storici**

## **Transparent Methods**

### **RESOURCE AVAILABILITY**

#### **Lead Contact**

Further information and requests for resources and reagents should be directed to and will be fulfilled by the Lead Contact, Francesca Storici (storici@gatech.edu).

#### **Materials Availability**

All unique/stable reagents generated in this study are available from the Lead Contact.

#### **Data and Code Availability**

The authors declare that the data supporting the findings of this study are available within the paper and its supplementary information files. The Ribose-Map bioinformatics toolkit is available for download at GitHub (<https://github.com/agombolay/ribose-map>). See also (Gombolay et al., 2019). Custom Python3 scripts for background subtraction is available for download at GitHub under GNU GPL v3.0 license (<https://github.com/xph9876/ArtificialRiboseDetection>). The custom Python3 scripts for heatmaps is available for download at GitHub under GNU GPL v3.0 license (<https://github.com/xph9876/RibosePreferenceAnalysis>)

Table S2 contains raw data. Bar graphs representing the percentage of each type of rNMP were made using GraphPad Prism 5 (GraphPad Software). The nucleotide sequence context plots were created using custom R scripts.

The datasets generated during this study are available at NCBI's SRA under BioProject ID PRJNA657931.

All data generated in this study are available from the Lead Contact.

### **EXPERIMENTAL MODEL AND SUBJECT DETAILS**

#### **Algal model growing culture and conditions**

The algae *Chlamydomonas reinhardtii* CC-1690 (wild type, mt+ strain) was obtained from the Chlamydomonas Resource Center at the University of Minnesota. Briefly, *C. reinhardtii* cells were grown in tris-acetate-phosphate medium (TAP) in a glass tube (5.1 cm width and 64 cm height) (Gorman and Levine, 1965). The culture was given continuous illumination from eleven 40-Watt 1.2 m long cool white, fluorescent light bulbs with a light path of approximately 7.6 cm, and sparged with air at ~1 L/min at room temperature (approximately 25 °C). The Cole-Parmer Model 300 pH/ORP meter (Cole-Parmer Instrument Co., Vernon Hills, IL) was used with a temperature controller, i.e., the Wahl Model C962 1/8-DIN Controller, which were connected to a solenoid; CO<sub>2</sub> was dosed periodically to maintain the pH at 8.0±0.2. *C. reinhardtii* cells were grown for 5-7 days to reach OD = 1.5-1.7 at 750 nm corresponding to 2x10<sup>6</sup> cells/mL. Small cultures for preparation of nucleotide or protein extracts were grown in TAP medium in the light for 3-4 days.

## **METHOD DETAILS**

### **dNTP and rNTP measurements**

*C. reinhardtii* cell lysates were prepared to extract the NTPs and rNTPs as described in (Diamond et al., 2004) with some modifications. Briefly, *C. reinhardtii* cells were grown in 20 mL of TAP medium in the light for 3-4 days, or in the dark for 10-12 days. Cells were harvested, washed with 1 x PBS, and resuspended in 65% ice-cold methanol and mixed by pipetting. Cells were then vortexed for 2 min and then heated to 95 °C for 3 min then placed on ice for 1 min. The cells were spun at 14,000 x g for 3 min. Aliquots were lyophilized and stored at -80 °C. We quantified the intracellular dNTPs and rNTPs using an ion pair chromatography-tandem mass spectrometry method (Fromentin et al., 2010) with some modifications. Chromatographic separation and detection were conducted on a Vanquish Flex system (Thermo Scientific, Waltham, MA) coupled with a TSQ Quantiva triple quadrupole mass spectrometer (Thermo Scientific, Waltham, MA). Analytes were separated using a Kinetex EVO-C18 column (100 X 2.1 mm, 2.6 µm) (Phenomenex, Torrance, CA) at a flow rate of 250 µL/min. The mobile phase A consisted of 2 mM of ammonium phosphate monobasic and 3 mM of hexylamine in water and the mobile phase B consisted of

acetonitrile. The LC gradient increased from 10% to 35% of mobile phase B in 5 min, and then returned to the initial condition. Selected reaction monitoring in both positive and negative modes (spray voltage: 3200 V (pos) or 2500 V (neg); sheath gas: 35 Arb; Auxiliary gas: 20 Arb; Ion transfer tube temperature: 350 °C; vaporizer temperature: 380 °C) was used to detect the targets: dATP (492→136, pos), dGTP (508→152, pos), dCTP (466→158.9, neg), TTP (481→158.9, neg), ATP (508→136, pos), GTP (524→152, pos), CTP (482→158.9, neg), UTP (483→158.9, neg). Extracted nucleotide samples were reconstituted in 100 µL of mobile phase A. After centrifuging at 13,800 x g for 10 min, 40 µL of supernatant was mixed with 10 µL of <sup>13</sup>C and <sup>15</sup>N labeled dNTPs and rNTPs as internal standards, and then subjected to analysis. Data were collected and processed by Thermo Xcalibur 3.0 software. Calibration curves were generated from nucleotide standards by serial dilutions in mobile phase A (dATP and dGTP 0.1 – 400 nM, dCTP and TTP 0.2 – 400 nM, rNTPs 1 – 4000 nM). The calibration curves had r<sup>2</sup> value greater than 0.99. All the chemicals and standards are analytical grade or higher and were obtained commercially from Sigma Aldrich (St. Louise, MO). Nucleotide standards were at least 98% pure.

### **Preparation of whole cells extracts**

*C. reinhardtii* cells were grown at room temperature for 3-4 days in the light in 20 mL of TAP media (ThermoFisher). The algae were collected by centrifugation at 10,000 x g for 1 min. The supernatant was removed, and the algae were washed with water and centrifuged again. The algae were resuspended in 400 µL of Algae Extraction buffer (60mM Na<sub>2</sub>CO<sub>3</sub>, 60mM DTT, 2% SDS, 12% sucrose) containing 1X cOmplete Mini, EDTA-free protease inhibitor cocktail (Roche, Milwaukee, WI). 100 µL of acid washed glass beads (425-600nm diameter) was added and then vortexed at 4 °C for 20 min. The supernatant was collected after centrifugation at 10,000 x g for 20 min at 4 °C. Aliquots were precipitated by the addition of 5 volumes of ice-cold acetone and incubated at -20 °C for 2 h. The precipitate was collected by centrifugation at 10,000 x g for 30 min at 4 °C and then air dried on ice. The dried proteins were resuspended in the appropriate buffer for further analysis. Coomassie stained gel of a 10% denaturing polyacrylamide gel was run at 120 volts for 90 min of the unpurified extraction and the purified extraction (see **Figure**

**S3A).** Bradford assay was performed on the purified sample indicating 0.9ug/ul of protein present. SDS in the unpurified sample prevented an accurate measurement of protein concentration.

#### **Assays to test cell extract activity to cleave at rNMPs in DNA**

Mixture of 2.5 pmol of Cy5 5' labeled oligonucleotide containing an RNMP (Cy5.3PS.rG or Cy5.3PS.rA) or the control DNA oligonucleotide (Cy5.3PS) and 3.75 pmol of complementary oligonucleotide (DNA.comp.3PS) in 1X Thermopol Reaction Buffer was heat denatured in boiling water for 5 min and cool down at room temperature to 30 °C to anneal the complementary oligonucleotides. 2.5 pmol of annealed oligonucleotide were incubated with 400 ng of *C. reinhardtii* protein extract, or just water as negative control, for 4 hours at room temperature. Successively, the mixture was treated with 9.95 ul of formamide (VWR, 0606-100ML) and incubated for 5 min at 95 °C to denature the double strand substrate, then the mixture was put on ice. The denatured substrate was mixed with 2.22 ul of 10X Orange Loading Dye (LICOR, C80809-01) and loaded on a 15% 7M urea denaturing polyacrylamide gel. As a positive control for this experiment, we used 5 units of *Escherichia coli* RNase HII (NEB, M0288L) in place of the *C. reinhardtii* protein extract. To test whether there was any inhibitory factor for RNase H2 activity present in the *C. reinhardtii* protein extract, we treated the 2.5 pmol of annealed oligonucleotide containing the rG with 5 units of *E. coli* RNase HII in the presence or absence of 400 ng of the *C. reinhardtii* protein extract.

#### **Algal Genomic DNA extraction and preparation**

After 5-7 days of growth in the presence of light, at a concentration of  $2 \times 10^6$  cells/mL, total DNA was isolated from 150 mL of algal cells grown in TAP medium as described in (Newman et al., 1990), with some modifications. Typically, algal cells were spun down at 3000 rpm corresponding to  $1,865 \times g$ , in three individual 50 mL sterile tubes and the pellets were resuspended in 500  $\mu$ L of dH<sub>2</sub>O and combined in one sterile tube (50 mL), and 3.0 mL of SDS elution buffer (SDS 2%, NaCl 400 mM, EDTA 40 mM, Tris-HCl 100 mM, adjust pH 8.0) was added. Algal genomic DNA was extracted three times using a

phenol/chloroform/isoamyl alcohol mixture (25:24:1) to eliminate all protein residues. Finally, the aqueous layer was extracted with chloroform: isoamyl alcohol (24:1). Algal genomic DNA was precipitated with isopropanol and washed with 70% cold ethanol. The pellet was air-dried overnight and dissolved in 200  $\mu$ L of RNase/DNase free water. Genomic DNA was stored at -20 °C for the construction of the ribose-seq libraries.

### **Ribose-seq library construction to map rNMPs in *C. reinhardtii* genomic DNA**

The ribose-seq libraries were prepared as previously described with some modifications (Balachander et al., 2020; Balachander et al., 2019). Extracted algal gDNA was fragmented using three different sets of restriction enzymes (SRE) all obtained from NEB: SREI (HaeIII, HincII, and PvuII), SREII (AfeI, AluI, and SspI), and SREIII (NaeI, PsiI, and RsaI). Each set of mixtures was incubated overnight at 37 °C to produce fragments of 500- to 3,000-bp gDNA with an average size of ~1.5 kb. Then, the fragments were tailed with dATP (Sigma-Aldrich) by Klenow fragment (3'→5' exo-) (NEB, Ipswich, MA) for 30 min at 37 °C. The resulting gDNA fragments were purified by QIAquick PCR Purification Kit (Qiagen) and then ligated to pre-annealed double-stranded adaptors that contain single dT overhangs and a unique molecular identifier (UMI) consisting of a randomized 8-base sequence containing a 3-base specific barcode by T4 DNA ligase (NEB) overnight at 15 °C. The resulting gDNA products were purified using RNAClean XP (Beckman Coulter). The adaptor-ligated DNA fragments were incubated in 0.3 M NaOH for 2 h at 55 °C to expose 2',3'-cyclic phosphate and 2'-phosphate termini of DNA at rNMP sites, followed by neutralization and purification by using RNAClean XP. The resulting single-stranded (ssDNA) products were incubated with AtRNL buffer (50 mM Tris-HCl, pH 7.5, 40 mM NaCl, 5 mM MgCl<sub>2</sub>, 1 mM DTT, 30  $\mu$ M ATP (Sigma-Aldrich) and 1  $\mu$ M AtRNL for 1 h at 30 °C, followed by purification using RNAClean XP. The resulting products were treated with T5 exonuclease (NEB) for 1.5 h at 37 °C to degrade the background of unligated, linear ssDNA, leaving self-ligated ssDNA circles intact. Then, the purification was performed by using RNAClean XP. Samples were successively treated with 1  $\mu$ M Tpt1, in Tpt buffer solution (20 mM Tris-HCl, pH 7.5, 5 mM MgCl<sub>2</sub>, 0.1 mM DTT, 0.4% Triton X-100), and 10 mM NAD<sup>+</sup> (Sigma-Aldrich)

for 1 h at 30 °C to remove the 2'-phosphate remaining at the ligation junction. After purification using RNAClean XP, the circular fragments were PCR-amplified using two rounds of amplifications to result in a ribose-seq library. A first round of PCR begins with an initial denaturation at 98 °C for 30 sec. Then denaturation at 98 °C for 10 sec, primer annealing at 65 °C for 30 sec, and DNA extension at 72 °C for 30 sec are performed; these 3 steps are repeated for 6 or 11 cycles. The 1st PCR round was performed to amplify and introduce the sequences of Illumina TruSeq CD Index primers. A second round of PCR begins with an initial denaturation at 98 °C for 30 sec. Then denaturation at 98 °C for 10 sec, primer annealing at 65 °C for 30 sec, and DNA extension at 72 °C for 30 sec are performed; these 3 steps are repeated for 9 or 11 cycles depending on the concentration of the circular ssDNAs containing the rNMPs. Successively, there is a final extension reaction at 72 °C for 2 min for both PCRs.

The primers (PCR.1 and PCR.2) (**Table S1**) used for the first PCR round were the same for all libraries. A second round of PCR was performed to attach specific indexes i7 and i5 for each library. The sequences of PCR primers and indexes can be found in **Table S1**. PCR round 1 and 2 were performed using Q5-High Fidelity polymerase (NEB) for 6 (FS231 and FS232) or 11 (FS121), and 9 (FS121) or 11 (FS231 and FS232) cycles, respectively. Following the PCR cycles, each ribose-seq library was loaded on a 6% non-denaturing polyacrylamide gel and stained using 1X SYBR Gold (Life Technologies) for 40 min. The ribose-seq product from several PCR reactions was selectively extracted to recover 200-700 bp to exclude any primer dimers and long products that are not proficient for sequencing. The DNA was recovered from the PAGE gel using the crush and soak method (Chen and Ruffner, 1996). The resulting ribose-seq libraries were mixed at equimolar concentrations and normalized to 1.5 nM. The libraries were sequenced on an Illumina NextSeq in the Molecular Evolution Core Facility at Georgia Institute of Technology.

**Processing and alignment of sequencing reads.** The sequencing reads consist of an eight-nucleotide UMI, a three-nucleotide molecular barcode, the tagged nucleotide (the nucleotide tagged during ribose-seq from which the position of the rNMP is determined), and the sequence directly downstream from the tagged

nucleotide. The UMI corresponds to sequencing cycles 1-6 and 10-11, the molecular barcode corresponds to cycles 7-9, the tagged nucleotide corresponds to cycle 12, and the tagged nucleotide's downstream sequence corresponds to cycles 13+ of the raw FASTQ sequences. The rNMP is the reverse complement of the tagged nucleotide. Before aligning the sequencing reads to the reference genome, the reads were trimmed based on sequencing quality and custom ribose-seq adaptor sequence using cutadapt 1.16 (-q 15 -m 62 -a 'AGTTGCGACACGGATCTATCA'). In addition, to ensure accurate alignment to the reference genome, reads containing fewer than 50 bases of genomic DNA (those bases located downstream from the tagged nucleotide) after trimming were discarded. Following quality control, the Alignment and Coordinate Modules of the Ribose-Map toolkit were used to process and analyze the reads (Gombolay et al., 2019). The Alignment Module de-multiplexed the trimmed reads by the appropriate molecular barcode, aligned the reads to the reference genome using Bowtie 2, and de-duplicated the aligned reads using UMI-tools. Based on the alignment results, the Coordinate Module filtered the reads to retain only those with a mapping quality score of at least 30 (probability of misalignment <0.001) and calculated the chromosomal coordinates and per-nucleotide counts of rNMPs. All ribose-seq libraries were then checked for background noise of restriction enzyme reads. We counted the number of reads ending with a restriction enzyme cut site, which is expected not to be generated by rNMP incorporation. Some reads captured the dAMP, which is added by dA-tailing at the restriction cut site. We summed up such background reads and calculated the percentage of background noise. All libraries had very low background (0.08% - 2.50%). To allow comparison between sequencing libraries of different read depth, the per-nucleotide coverage was calculated by normalizing raw rNMP counts to counts per hundred. The FASTQ files used as input into the Ribose-Map toolkit are available upon request.

**Nucleotide sequence context of embedded rNMPs.** Using the Sequence Module of Ribose-Map, the frequencies of the nucleotides at rNMP sites and 100 nucleotides upstream and downstream from those sites were calculated for the mitochondrial, chloroplast and nuclear genomes of *C. reinhardtii*. The



Sequence Module normalizes the nucleotide frequencies to the frequencies of the corresponding reference genome.

**Identification of genes for RNase H2 subunits A, B and C in the genome of *C. reinhardtii*.** To identify genes for RNase H2 subunits A, B and C in the genome of *C. reinhardtii*, we have used a gene finder GeneMark-EP+ (Bruna et al., 2020). The gene finder was run on the *C. reinhardtii* genome (v 5.5) to identify genes encoding homologs of RNase H2 subunits. As a source of external evidence for running GeneMark-EP+ and its protein mapping pipeline ProtHint, we used i/ OrthoDB segment of plant proteins as well as ii/ amino acid sequences of the three families of subunits A, B and C of RNase H2, particularly 1,059 subunits A, 719 subunits B and 662 subunits C, available in the NCBI protein database.

**Heatmaps.** To generate the mononucleotide heatmaps for every mitochondrial, chloroplast and nuclear ribose-seq library, the number of each type of rNMP ( $R_N$ :  $R_A$ ,  $R_C$ ,  $R_G$  or  $R_U$ ) was counted and divided by the

$$R_{N_R,raw} = \frac{R_N}{R_A + R_C + R_G + R_U}$$

total number of rNMPs to yield the proportion  $R_{N_R,raw}$ :

Then, each raw counts of rNMPs ( $R_N$ ) was divided by the corresponding deoxy-mononucleotide frequency of the reference genome ( $N_N$ ) to yield the probability of rNMP incorporation  $P_{R_N}$ , and were normalized to generate the normalized proportion  $R_{R_N,norm}$ . These data were used in the normalized mononucleotide heatmaps:

$$P_{R_N} = \frac{R_N}{N_N} \quad R_{R_N,norm} = \frac{P_{R_N}}{P_{R_A} + P_{R_C} + P_{R_G} + P_{R_U}}$$

Similarly, to generate the normalized dinucleotide heatmaps, each raw count of dinucleotides with an rNMP along with a deoxyribonucleotide at position -1, -2, -3, -4, -5, -6 or -100 relative to the rNMP ( $R_{NR}$ ), or at position +1, +2, +3, +4, +5, +6 or +100 relative to the rNMP ( $R_{RN}$ ) were divided by the corresponding deoxy-dinucleotide frequency of the reference genome ( $N_{NN}$ ) to yield the probability of NR and RN

dinucleotide incorporation  $P_{R_{NR}}$  and  $P_{R_{RN}}$ , respectively. Next, these proportions were normalized keeping fixed the deoxyribonucleotide base in the position of the rNMP to generate the normalized proportion

$$R_{R_{NR},norm} \text{ or } R_{R_{RN},norm}: \quad P_{R_{NR}} = \frac{R_{NR}}{N_{NN}} \quad R_{R_{NR},norm} = \frac{P_{R_{NR}}}{P_{R_{AR}} + P_{R_{CR}} + P_{R_{GR}} + P_{R_{TR}}}$$

$$P_{R_{RN}} = \frac{R_{RN}}{N_{NN}} \quad R_{R_{RN},norm} = \frac{P_{R_{RN}}}{P_{R_{RA}} + P_{R_{RC}} + P_{R_{RG}} + P_{R_{RT}}}$$

The specific background frequencies of mononucleotides and dinucleotides for mitochondrial, chloroplast and nuclear DNA are shown in the heatmap figures.

## QUANTIFICATION AND STATISTICAL ANALYSIS

**Statistical analysis for heatmaps.** To compare NTP/dNTP ratios shown in **Figure 1B**, we used the t-test.

The Chi-square test is used for analyses of heatmap data to check if the rNMPs are uniformly distributed, as described in the legend of **Table S3**.

## SUPPLEMENTAL REFERENCES

- Balachander, S., Gombolay, A.L., Yang, T., Xu, P., Newnam, G., Keskin, H., El-Sayed, W.M.M., Bryksin, A.V., Tao, S., Bowen, N.E., *et al.* (2020). Ribonucleotide incorporation in yeast genomic DNA shows preference for cytosine and guanosine preceded by deoxyadenosine. *Nat Commun* *11*, 2447.
- Balachander, S., Yang, T., Newnam, G., El-Sayed, W.M.M., Koh, K.D., and Storici, F. (2019). Capture of Ribonucleotides in Yeast Genomic DNA Using Ribose-Seq. *Methods Mol Biol* *2049*, 17-37.
- Bruna, T., Lomsadze, A., and Borodovsky, M. (2020). GeneMark-EP+: eukaryotic gene prediction with self-training in the space of genes and proteins. *NAR Genom Bioinform* *2*, lqaa026.
- Chen, Z., and Ruffner, D.E. (1996). Modified crush-and-soak method for recovering oligodeoxynucleotides from polyacrylamide gel. *Biotechniques* *21*, 820-822.
- Diamond, T.L., Roshal, M., Jamburuthugoda, V.K., Reynolds, H.M., Merriam, A.R., Lee, K.Y., Balakrishnan, M., Bambara, R.A., Planelles, V., Dewhurst, S., *et al.* (2004). Macrophage tropism of HIV-1 depends on efficient cellular dNTP utilization by reverse transcriptase. *J Biol Chem* *279*, 51545-51553.
- Fromentin, E., Gavegnano, C., Obikhod, A., and Schinazi, R.F. (2010). Simultaneous quantification of intracellular natural and antiretroviral nucleosides and nucleotides by liquid chromatography-tandem mass spectrometry. *Anal Chem* *82*, 1982-1989.
- Gombolay, A.L., Vannberg, F.O., and Storici, F. (2019). Ribose-Map: a bioinformatics toolkit to map ribonucleotides embedded in genomic DNA. *Nucleic Acids Res* *47*, e5.
- Gorman, D.S., and Levine, R.P. (1965). TAP and Tris-minimal medium. *Proc Natl Acad Sci USA* *54*, 1665-1669.
- Newman, S.M., Boynton, J.E., Gillham, N.W., Randolph-Anderson, B.L., Johnson, A.M., and Harris, E.H. (1990). Transformation of chloroplast ribosomal RNA genes in *Chlamydomonas*: molecular and genetic characterization of integration events. *Genetics* *126*, 875-888.

# Figure S1

**A**

Sample	Concentration of dNTPs and rNTPS: pmols per 10 <sup>7</sup> cells							
<i>C. reinhardtii</i>	rATP	rCTP	rGTP	rUTP	dATP	dCTP	dGTP	dTTP
1	258.6	11.3	40.0	13.3	0.146	0.026	0.186	0.076
2	198.1	4.81	37.7	8.65	0.115	0.024	0.104	0.073
3	152.3	3.24	32.5	7.47	0.082	0.026	0.136	0.065
4	174.9	3.64	37.8	10.5	0.104	0.041	0.129	0.062

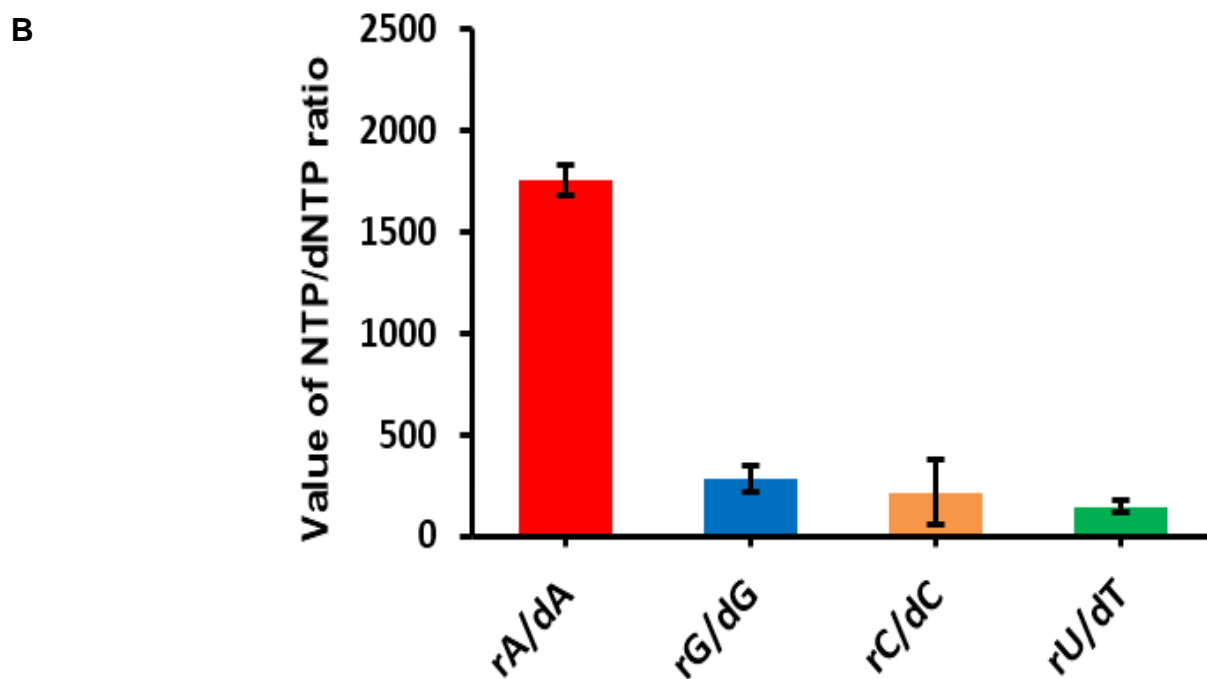


**Figure S1. Measurements of NTP and dNTP levels in *C. reinhardtii* cells growing in the dark, Related to Figure 1.** (A) The levels of NTPs and dNTPs extracted from known numbers of algal cells of *C. reinhardtii* strain CC-1690 grown in the dark were determined by LC-MS/MS methods (see Methods). The cellular level of each nucleotide was normalized for 10<sup>7</sup> cells. (B) The NTP and dNTP levels determined in A) were used to calculate the NTP/dNTP ratios. Shown are mean and standard deviation of four repeats for each sample.

**Figure S2**

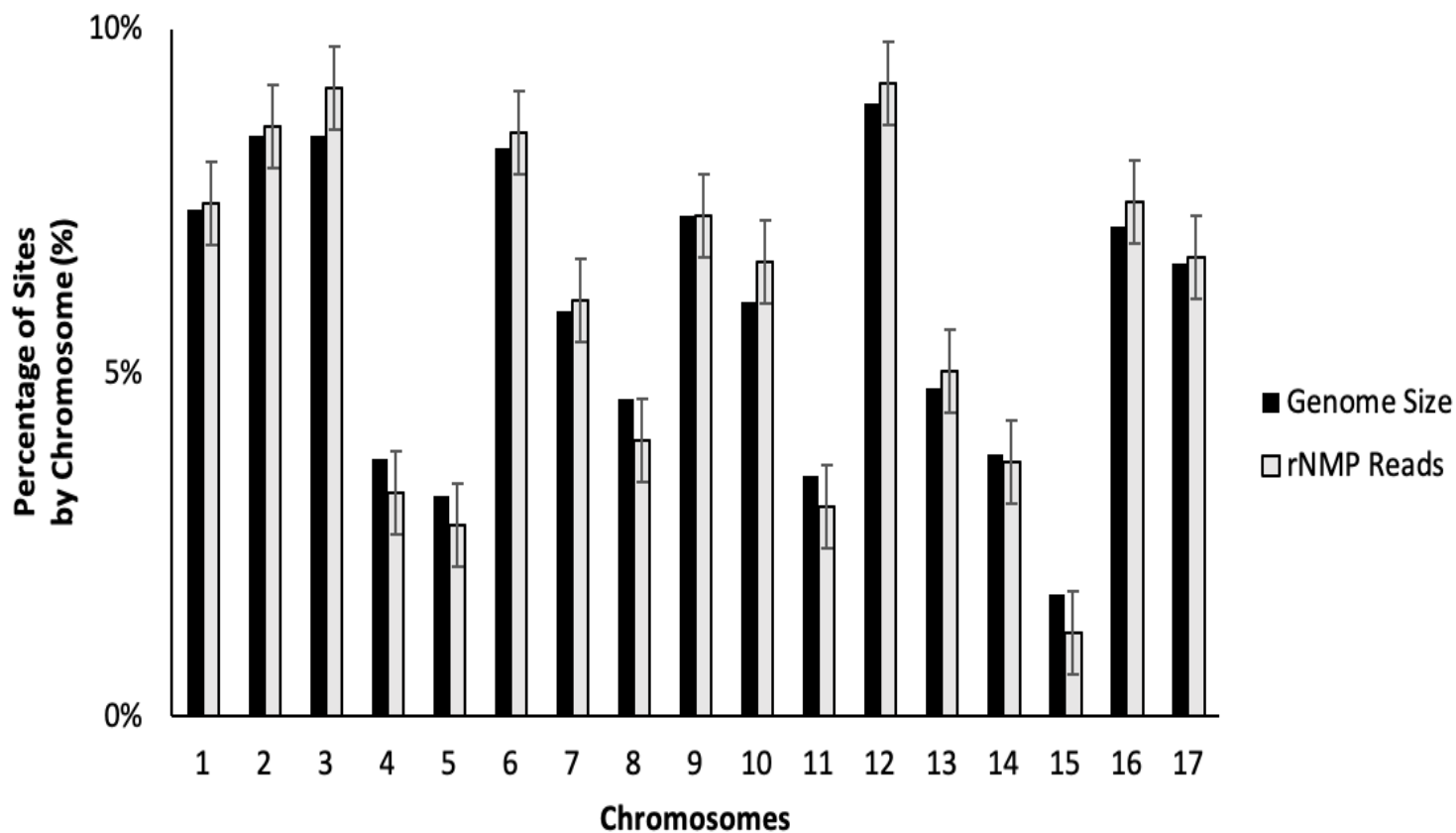
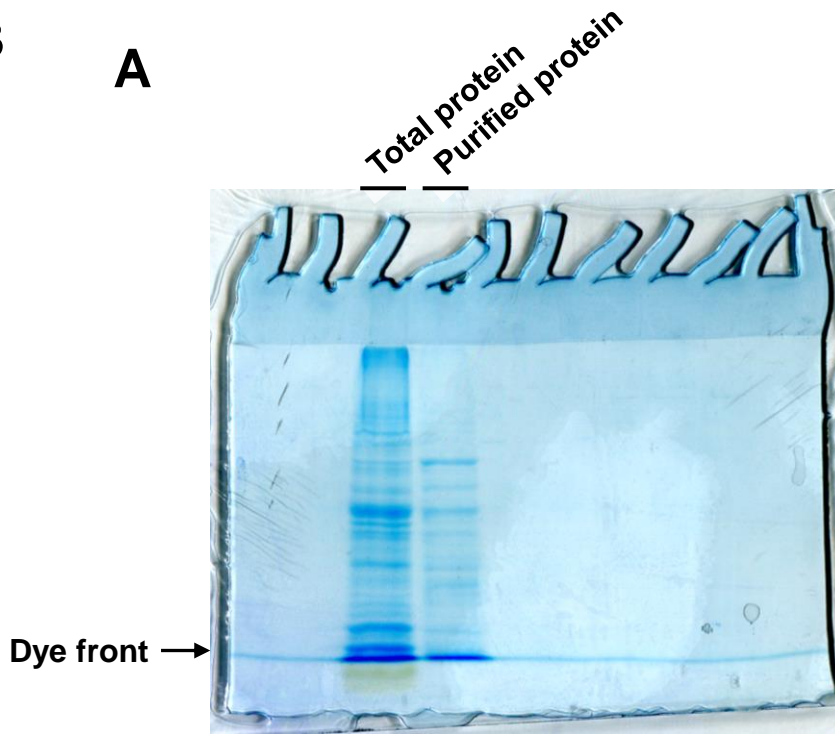


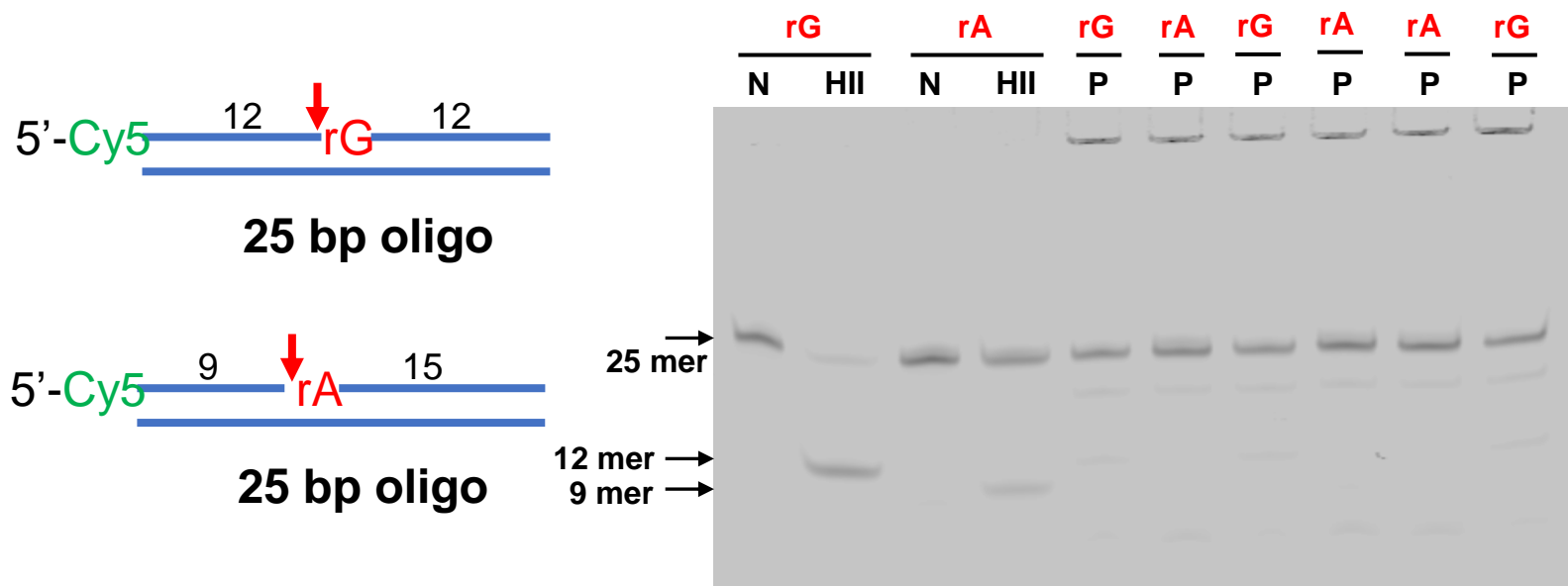
**Figure S2. Chromosomal distribution of rNMPs compared to size of each nuclear chromosome, Related to Figure 2.** Percentage of rNMP sites were calculated for each nuclear chromosome and plotted against the size of each chromosome for comparison.

**Figure S3**

**A**



**B**



**C**

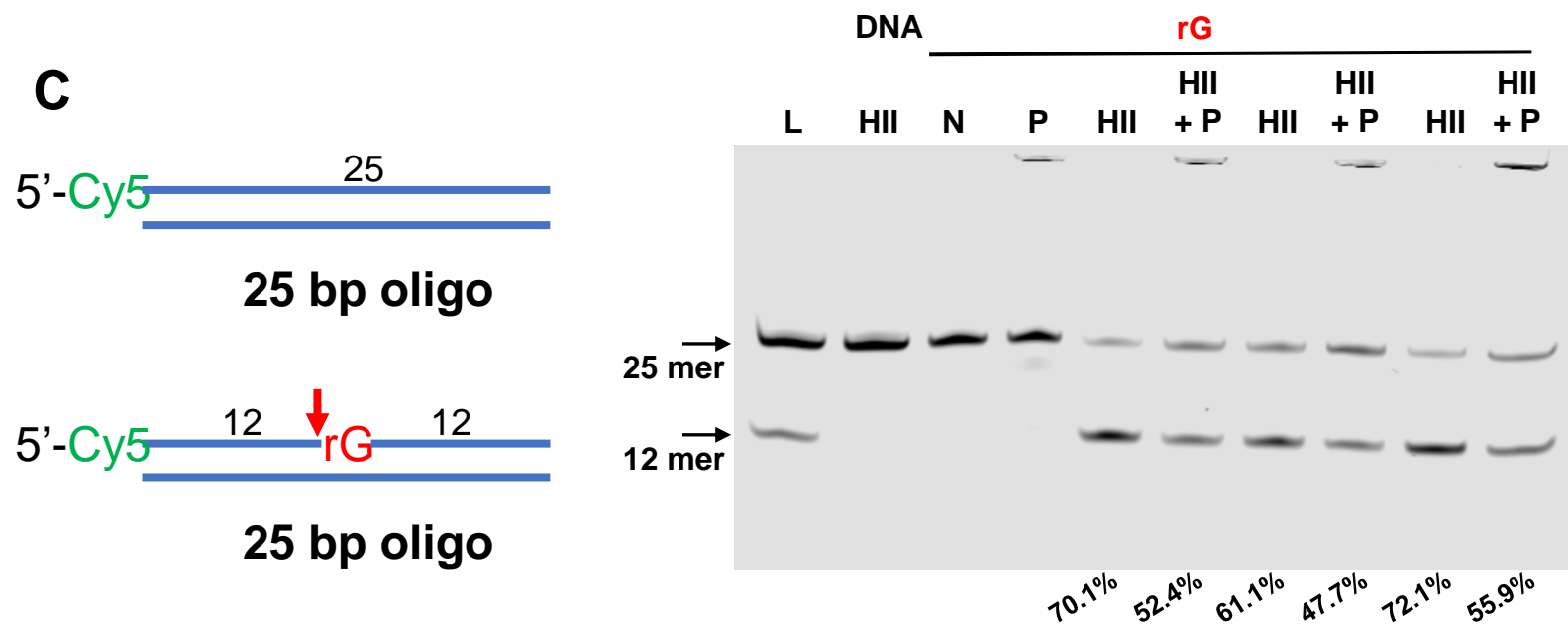
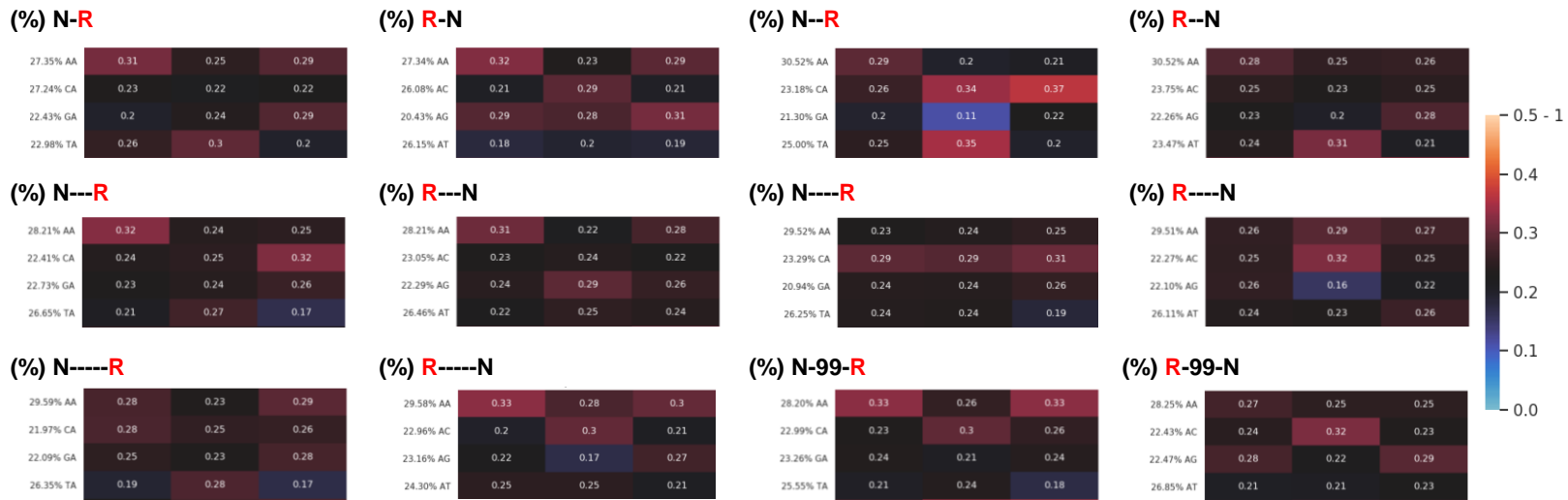


**Figure S3. Protein extract from *C. reinhardtii* do not cleave at rNMPs in DNA, Related to Figure 2.** (A) Coomassie stained gel of a 10% denaturing polyacrylamide gel was run at 120 volts for 90 min of the unpurified extraction and the purified extraction. The first lane contains 10ul of unpurified protein in extraction buffer containing 1X cOmplete Mini, EDTA-free protease inhibitor cocktail (Roche) while the second lane is 10ul of purified extract via acetone precipitation. (B) Double-stranded Cy5-labeled 25-mers containing an rNMP (rG or rA) were used in the *in vitro* cleavage assay to test RNase H2 activity in *C. reinhardtii* protein extracts, schemes shown to the left. The red arrow shows the cleavage position by RNase HII/2. N, negative control with the double-stranded oligonucleotide (with rG or rA, as indicated) treated by water. HII, *Escherichia coli* RNase HII was used as a positive control cleaving 5' of the rNMP embedded in the double stranded DNA oligonucleotides. P, *C. reinhardtii* protein extract. (C) *E. coli* RNase HII (HII) and *C. reinhardtii* protein extract (P) were combined (HII + P) to test any inhibitory effect of P on RNase H activity on the rG-containing substrate (shown on the left). DNA, negative control double-stranded, DNA-only, Cy5-labeled 25-mer (shown on the left). L, ladder with 25mer and 12mer bands. N, negative control with the double-stranded oligonucleotide with rG treated by water. The cleavage % is shown underneath the image.

# Figure S4

## A

### Dinucleotide ratios normalized to background frequency in mitochondria



## B

### Dinucleotide ratios normalized to background frequency in chloroplast

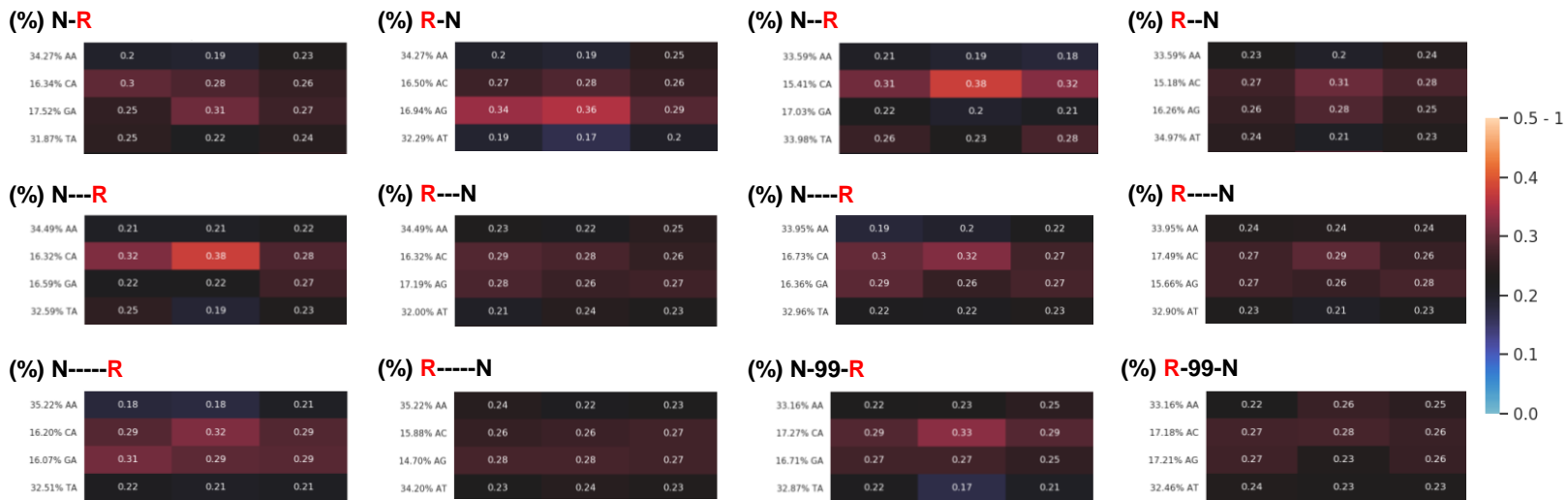


**Figure S4.** Like the +1, the deoxyribonucleotide at positions -2 to -6, and +2 to +6 have less impact than the one immediately upstream (-1) on rAMP occurrence in *C. reinhardtii* mitochondrial and chloroplast DNA, Related to Figures 4 and 5. Heatmap analyses with normalized frequency of N-R, R-N, N--R, R--N, N---R, R---N, N----R, R----N, N-----R, R-----N, N-99-R, and R-99-N dinucleotides (rA with the -2, +2, -3, +3, -4, +4, -5, +5, -6, +6, -100 or +100 deoxyribonucleotide with base A, C, G or T) for all the mitochondrial (A) and chloroplast (B) ribose-seq libraries of this study. The formulas used to calculate these normalized frequencies are shown and explained in Materials and Methods. Each column of the heatmaps shows results of a specific ribose-seq library. Each library name is indicated underneath each column of the heatmaps. Each row shows results obtained for a dinucleotide RN, N-R, R-N, N--R, R--N, N---R, R---N, N----R, R----N, N-----R, R-----N, N-99-R, or R-99-N of fixed rNMP base A for each library. The actual % of dinucleotides of fixed base A for the indicated base combinations that are present in mitochondrial (A) or chloroplast (B) DNA of *C. reinhardtii* are shown to the left of the heatmaps. The observed % of dinucleotides with rNMPs with base A were divided by the actual % of each dinucleotide with fixed base A in mitochondrial or chloroplast DNA of *C. reinhardtii*. The bar to the right shows how different frequency values are represented as different colors. Black corresponds to 0.25.



# Figure S5

## Dinucleotide ratios normalized to background frequency in nucleus

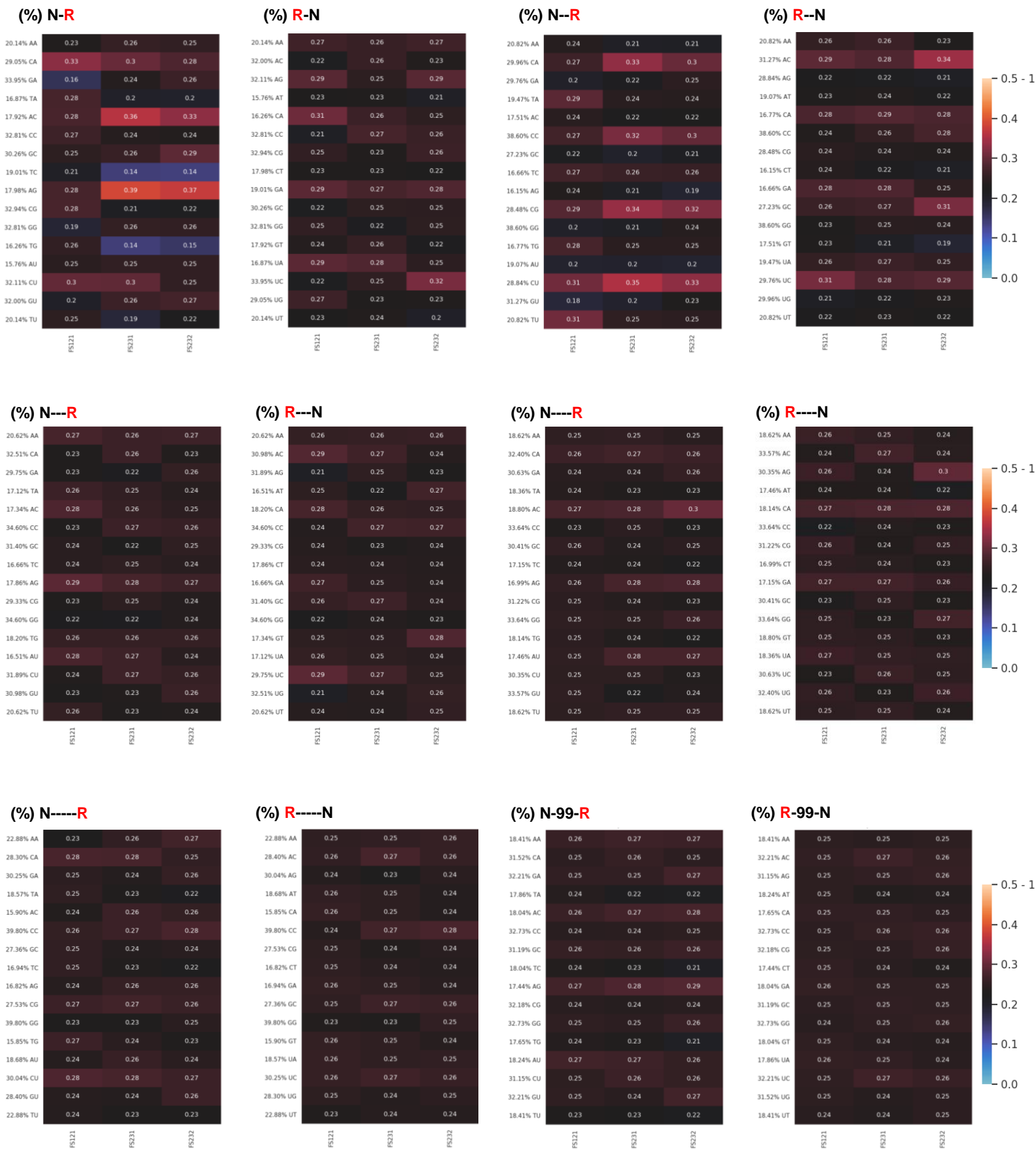


**Figure S5.** Like the +1, the deoxyribonucleotide immediately downstream (+1) from each rNMP and those at positions -2 to -6, and +2 to +6 have less impact than the one immediately upstream (-1) on rNMP occurrence in *C. reinhardtii* nuclear DNA, Related to **Figure 6**. Heatmap analyses with normalized frequency of N-R, R-N, N--R, R--N, N---R, R---N, N----R, R----N, N-----R, R-----N, N-99-R, and R-99-N dinucleotides (rA, rC, rG, or rU with the -2, +2, -3, +3, -4, +4, -5, +5, -6, +6, -100 or +100 deoxyribonucleotide with base A, C, G or T) for all the nuclear ribose-seq libraries of this study. The formulas used to calculate these normalized frequencies are shown and explained in Materials and Methods. Each column of the heatmaps shows results of a specific ribose-seq library. Each library name is indicated underneath each column of the heatmaps. Each row shows results obtained for a dinucleotide RN, N-R, R-N, N--R, R--N, N---R, R---N, N----R, R----N, N-----R, R-----N, N-99-R, or R-99-N of fixed rNMP base A, C, G or U for each library. The actual % of dinucleotides of fixed base A, C, G or T for the indicated base combinations that are present in nuclear DNA of *C. reinhardtii* are shown to the left of the heatmaps. The observed % of dinucleotides with NMPs with base A, C, G or U were divided by the actual % of each dinucleotide with fixed base A, C, G or T in nuclear DNA of *C. reinhardtii*. The bar to the right shows how different frequency values are represented as different colors. Black corresponds to 0.25.

**Table S1. Oligonucleotides used in this study, Related to Figure 2**

Name	Size	Sequence
Adaptor.L1	65	5' P-NNC CGN NNN NNA GAT CGG AAG AGC GTC GTG TAG GGA AAG AGT GTT GAT AGA TCC GTG TCG CAA CT
Adaptor.L2	65	5' P-NNT GAN NNN NNA GAT CGG AAG AGC GTC GTG TAG GGA AAG AGT GTT GAT AGA TCC GTG TCG CAA CT
Adaptor.S	25	5' P-GTT GCG ACA CGG ATC TAT CAA CAC T -Am
PCR.1	54	5' GTG ACT GGA GTT CAG ACG TGT GCT CTT CCG ATC TTG ATA GAT CCG TGT CGC AAC
PCR.2	20	5' ACA CTC TTT CCC TAC ACG AC
PCR.701	53	5' CAA GCA GAA GAC GGC ATA CGA GAT <b>CGA GTA ATG</b> TGA CTG GAG TTC AGA CGT GT
PCR.702	53	5' CAA GCA GAA GAC GGC ATA CGA GAT <b>TCT CCG GAG</b> TGA CTG GAG TTC AGA CGT GT
PCR.707	53	5' CAA GCA GAA GAC GGC ATA CGA GAT <b>AGC TTC AGG</b> TGA CTG GAG TTC AGA CGT GT
PCR.502	57	5' AAT GAT ACG GCG ACC GAG ATC TAC ACA <b>TAG AGG CAC</b> ACT CTT TCC CTA CAC GAC
PCR.507	57	5' AAT GAT ACG GCG ACC GAG ATC TAC ACC <b>AGG ACG TAC</b> ACT CTT TCC CTA CAC GAC
PCR.508	57	5' AAT GAT ACG GCG ACC GAG ATC TAC ACG <b>TAC TGA CAC</b> ACT CTT TCC CTA CAC GAC
Cy5.3PS.rG	25	5'/5Cy5/G*G*A*TCCGGTAGT <b>rG</b> TTAGGCCTG*A*A*C (* phosphorothioate linkage)
Cy5.3PS.rA	25	5'/5Cy5/G*G*A*TCCGGT <b>rA</b> GTGTTAGGCCTG*A*A*C (* phosphorothioate linkage)
Cy5.3PS	25	5'/Cy5/G*G*A*TCCGGTAGT <b>G</b> TTAGGCCTG*A*A*C (* phosphorothioate linkage)

DNA.comp.3PS	25	5' <b>G</b> *T*T*CAGGCCTAACACTACCGGA*T*C*C (* phosphorothioate linkage)
--------------	----	--

Name, length, and sequence of oligonucleotides used in this study are presented. All bold letters in the PCR primers indicate the specific sequence of index used in sequencing. 'P and Am' indicate end modifications of phosphate and amino groups, respectively. Oligonucleotides Cy5.3PS.rG, Cy5.3PS.rA, Cy5.3PS and DNA.comp.3PS were used in the *in vitro* cleavage experiments. The rNMP is shown in red, bolded text. The asterisks indicate phosphorothioate linkages. The oligos were prepared by IDT, purified by RNase free HPLC. All oligonucleotides were desalted, except the first three listed (Adaptors), which were HPLC purified.